113. Supersymmetry, Part II (Experiment)

Updated September 2017 by O. Buchmueller (Imperial College London) and P. de Jong (Nikhef and University of Amsterdam).

113.1. Introduction

Supersymmetry (SUSY), a transformation relating fermions to bosons and vice versa [1–9], is one of the most compelling possible extensions of the Standard Model of particle physics (SM).

On theoretical grounds SUSY is motivated as a generalization of space-time symmetries. A low-energy realization of SUSY, *i.e.*, SUSY at the TeV scale, is, however, not a necessary consequence. Instead, low-energy SUSY is motivated by the possible cancellation of quadratic divergences in radiative corrections to the Higgs boson mass [10–15]. Furthermore, it is intriguing that a weakly interacting, (meta)stable supersymmetric particle might make up some or all of the dark matter in the universe [16–18]. In addition, SUSY predicts that gauge couplings, as measured experimentally at the electroweak scale, unify at an energy scale $\mathcal{O}(10^{16})$ GeV ("GUT scale") near the Planck scale [19–25].

In the minimal supersymmetric extension to the Standard Model, the so called MSSM [11,26,27], a supersymmetry transformation relates every fermion and gauge boson in the SM to a supersymmetric partner with half a unit of spin difference, but otherwise with the same properties (such as mass) and quantum numbers. These are the "sfermions": squarks ($\tilde{q}$) and sleptons ($\tilde{\ell}$, $\tilde{\nu}$), and the "gauginos". The MSSM Higgs sector contains two doublets, for up-type quarks and for down-type quarks and charged leptons respectively. After electroweak symmetry breaking, five Higgs bosons arise, of which two are charged. The supersymmetric partners of the Higgs doublets are known as "higgsinos." The weak gauginos and higgsinos mix, giving rise to charged mass eigenstates called "charginos" ($\tilde{\chi}^{\pm}$), and neutral mass eigenstates called "neutralinos" ($\tilde{\chi}^{0}$). The SUSY partners of the gluons are known as "gluinos" ($\tilde{g}$). The fact that such

particles are not yet observed leads to the conclusion that, if supersymmetry is realized, it is a broken symmetry. A description of SUSY in the form of an effective Lagrangian with only "soft" SUSY breaking terms and SUSY masses at the TeV scale maintains cancellation of quadratic divergences in particle physics models.

The phenomenology of SUSY is to a large extent determined by the SUSY breaking mechanism and the SUSY breaking scale. This determines the SUSY particle masses, the mass hierarchy, the field contents of physical particles, and their decay modes. In addition, phenomenology crucially depends on whether the multiplicative quantum number of R-parity [27], $R = (-1)^{3(B-L)+2S}$, where B and L are baryon and lepton numbers and S is the spin, is conserved or violated. If R-parity is conserved, SUSY particles (sparticles), which have odd R-parity, are produced in pairs and the decays of each SUSY particle must involve an odd number of lighter SUSY particles. The lightest SUSY particle (LSP) is then stable and often assumed to be a weakly interacting massive particle (WIMP). If R-parity is violated, new terms λ_{ijk}, λ'_{ijk} and λ''_{ijk} appear in the superpotential, where ijk are generation indices; λ-type couplings appear between lepton superfields only, λ''-type are between quark superfields only, and λ'-type couplings connect the two. R-parity violation implies lepton and/or baryon number violation. More details of the theoretical framework of SUSY are discussed elsewhere in this volume [28].

Today, low-energy data from flavor physics experiments, high-precision electroweak observables as well as astrophysical data impose strong constraints on the allowed SUSY parameter space. Recent examples of such data include measurements of the rare B-meson decay $B_s \to \mu^+\mu^-$ [29,30], measurements of the anomalous magnetic moment of the muon [31], and accurate determinations of the cosmological dark matter relic density constraint [32,33].

These indirect constraints are often more sensitive to higher SUSY mass scales than experiments searching for direct sparticle production at colliders, but the interpretation of these results is often strongly model dependent. In contrast, direct searches for sparticle production at collider experiments are less subject to interpretation ambiguities and therefore they play a crucial role in the search for SUSY.

The discovery of a Higgs boson with a mass around 125 GeV imposes constraints on SUSY, which are discussed elsewhere [28,34].

In this review we limit ourselves to direct searches, covering data analyses at LEP, HERA, the Tevatron and the LHC, with emphasis on the latter. For more details on LEP and Tevatron constraints, see earlier PDG reviews [35].

113.2. Experimental search program

The electron-positron collider LEP was operational at CERN between 1989 and 2000. In the initial phase, center-of-mass energies around the Z-peak were probed, but after 1995 the LEP experiments collected a significant amount of luminosity at higher center-of-mass energies, some 235 pb^{-1} per experiment at $\sqrt{s} \geq 204$ GeV, with a maximum $\sqrt{s}$ of 209 GeV.

Searches for new physics at e^+e^- colliders benefit from the clean experimental environment and the fact that momentum balance can be measured not only in the plane

transverse to the beam, but also in the direction along the beam (up to the beam pipe holes), defined as the longitudinal direction. Searches at LEP are dominated by the data samples taken at the highest center-of-mass energies.

Constraints on SUSY have been set by the CDF and D0 experiments at the Tevatron, a proton-antiproton collider at a center-of-mass energy of up to 1.96 TeV. CDF and D0 have collected integrated luminosities between 10 and 11 fb^{-1} each up to the end of collider operations in 2011.

The electron-proton collider HERA provided collisions to the H1 and ZEUS experiments between 1992 and 2007, at a center-of-mass energy up to 318 GeV. A total integrated luminosity of approximately 0.5 fb^{-1} was collected by each experiment. Since in ep collisions no annihilation process takes place, SUSY searches at HERA typically look for R-parity violating production of single SUSY particles.

The Large Hadron Collider (LHC) at CERN started proton-proton operation at a center-of-mass energy of 7 TeV in 2010. By the end of 2011 the experiments ATLAS and CMS had collected about 5 fb^{-1} of integrated luminosity each, and the LHCb experiment had collected approximately 1 fb^{-1}. In 2012, the LHC operated at a center-of-mass energy of 8 TeV, and ATLAS and CMS collected approximately 20 fb^{-1} each, whereas LHCb collected 2 fb^{-1}. In 2015, the LHC started Run 2, with a center-of-mass energy of 13 TeV. At the end of 2016, ATLAS and CMS had both collected approximately 36 fb^{-1}, and LHCb had collected 2 fb^{-1}.

Proton-(anti)proton colliders produce interactions at higher center-of-mass energies than those available at LEP, and cross sections of QCD-mediated processes are larger, which is reflected in the higher sensitivity for SUSY particles carrying color charge: squarks and gluinos. Large background contributions from Standard Model processes, however, pose challenges to trigger and analysis. Such backgrounds are dominated by multijet production processes, including, particularly at the LHC, those of top quark production, as well as jet production in association with vector bosons. The proton momentum is shared between its parton constituents, and in each collision only a fraction of the total center-of-mass energy is available in the hard parton-parton scattering. Since the parton momenta in the longitudinal direction are not known on an event-by-event basis, use of momentum conservation constraints in an analysis is restricted to the transverse plane, leading to the definition of transverse variables, such as the missing transverse momentum, and the transverse mass. Proton-proton collisions at the LHC differ from proton-antiproton collisions at the Tevatron in the sense that there are no valence anti-quarks in the proton, and that gluon-initiated processes play a more dominant role. The increased center-of-mass energy of the LHC compared to the Tevatron, as well as the increase at the LHC between Run 1 and Run 2, significantly extends the kinematic reach for SUSY searches. This is reflected foremost in the sensitivity for squarks and gluinos, but also for other SUSY particles.

The main production mechanisms of massive colored sparticles at hadron colliders are squark-squark, squark-gluino and gluino-gluino production; when "squark" is used "antisquark" is also implied. The typical SUSY search signature at hadron colliders contains high-p_{T} jets, which are produced in the decay chains of heavy squarks and gluinos, and significant missing momentum originating from the two LSPs produced at

the end of the decay chain. Assuming R-parity conservation, the LSPs are expected to be neutral and weakly interacting massive particles, since otherwise the model contradicts standard cosmology. These particles then escape detection at colliders. Standard Model backgrounds with missing transverse momentum include leptonic W/Z-boson decays, heavy-flavor decays to neutrinos, and multijet events that may be affected by instrumental effects such as jet mismeasurement.

Selection variables designed to separate the SUSY signal from the Standard Model backgrounds include H_{T}, $E_{\mathrm{T}}^{\mathrm{miss}}$, and m_{eff}. The quantities H_{T} and $E_{\mathrm{T}}^{\mathrm{miss}}$ refer to the measured transverse energy and missing transverse momentum in the event, respectively. They are usually defined as the scalar sum of the transverse jet momenta or calorimeter clusters transverse energies measured in the event (H_{T}), or the negative vector sum of transverse momenta of reconstructed objects like jets and leptons in the event ($E_{\mathrm{T}}^{\mathrm{miss}}$). The quantity m_{eff} is referred to as the effective mass of the event and is defined as $m_{\mathrm{eff}} = H_{\mathrm{T}} + |E_{\mathrm{T}}^{\mathrm{miss}}|$. The peak of the m_{eff} distribution for SUSY signal events correlates with the SUSY mass scale, in particular with the mass difference between the primary produced SUSY particle and the LSP [36], whereas the Standard Model backgrounds dominate at low m_{eff}. Additional reduction of multijet backgrounds can be achieved by demanding isolated leptons or photons in the final states; in such events the lepton or photon transverse momentum may be added to H_{T} or m_{eff} for further signal-background separation.

At the LHC, alternative approaches have been developed to increase the sensitivity to pair production of heavy sparticles with TeV-scale masses focusing on the kinematics of their decays, and to further suppress the background from multijet production. Prominent examples of these new approaches are searches using the α_{T} [37–41], *razor* [42], *stransverse mass* (m_{T2}) [43], and *contransverse mass* (m_{CT}) [44] variables. Recently, the topological event reconstruction methods have expanded with the *super-razor* [45] and *recursive jigsaw reconstruction* [46] techniques. Furthermore, frequently the searches for massive SUSY particles attempt to identify their decay into top quarks or vector bosons, which are themselves unstable. If these are produced with a significant boost, jets from their decay will typically overlap, and such topologies are searched for with *jet-substructure* [47] techniques.

113.3. Interpretation of results

Since the mechanism by which SUSY is broken is unknown, a general approach to SUSY via the most general soft SUSY breaking Lagrangian adds a significant number of new free parameters. For the minimal supersymmetric standard model, MSSM, *i.e.*, the model with the minimal particle content, these comprise 105 new parameters. A phenomenological analysis of SUSY searches leaving all these parameters free is not feasible. For the practical interpretation of SUSY searches at colliders several approaches are taken to reduce the number of free parameters.

One approach is to assume a SUSY breaking mechanism and lower the number of free parameters through the assumption of additional constraints. Before the start of the LHC, interpretations of experimental results were predominately performed in

constrained models of gravity mediated [48,49], gauge-mediated [50–52], and anomaly mediated [53,54] SUSY breaking. The most popular model was the constrained MSSM (CMSSM) [48,55,56], which in the literature is also referred to as minimal supergravity, or MSUGRA.

These constrained SUSY models are theoretically well motivated and provide a rich spectrum of experimental signatures. However, with universality relations imposed on the soft SUSY breaking parameters, they do not cover all possible kinematic signatures and mass relations of SUSY. In such scenarios the squarks are often nearly degenerate in mass, in particular for the first and second generation. The exclusion of parameter space in the CMSSM and in CMSSM-inspired models is mainly driven by first and second generation squark production together with gluino production. As shown in Fig. 113.1 [57] these processes possess the largest production cross sections in proton-proton collisions, and thus the LHC searches typically provide the tightest mass limits on these colored sparticles. This, however, implies that the allowed parameter space of constrained SUSY models today has been restrained significantly by searches from ATLAS and CMS. Furthermore, confronting the remaining allowed parameter space with other collider and non-collider measurements, which are directly or indirectly sensitive to contributions from SUSY, the overall compatibility of these models with all data is significantly worse than in the pre-LHC era (see section II.8 for further discussion), indicating that very constrained models like the CMSSM are no longer be good benchmark scenarios to solely characterize the results of SUSY searches at the LHC.

For these reasons, an effort has been made in the past years to complement the traditional constrained models with more flexible approaches.

One approach to study a broader and more comprehensive subset of the MSSM is via the phenomenological-MSSM, or pMSSM [60–62]. It is derived from the MSSM, using experimental data to eliminate parameters that are free in principle but have already been highly constrained by measurements of *e.g.*, flavor mixing and CP-violation. This effective approach reduces the number of free parameters in the MSSM to typically 19 or even less, making it a practical compromise between the full MSSM and highly constrained models such as the CMSSM.

Even less dependent on fundamental assumptions are interpretations in terms of so-called simplified models [63–66]. Such models assume a limited set of SUSY particle production and decay modes and leave open the possibility to vary masses and other parameters freely. Therefore, simplified models enable comprehensive studies of individual SUSY topologies, and are useful for optimization of the experimental searches over a wide parameter space without limitations on fundamental kinematic properties such as masses, production cross sections, and decay modes.

As a consequence, ATLAS and CMS have adopted simplified models as the primary framework to provide interpretations of their searches. In addition to using simplified models that describe prompt decays of SUSY particles, the experiments are now also focusing more on the use simplified models that allow for decays of long-lived SUSY particles as they can arise in different SUSY scenarios (see section II.7 for further discussion). Today, almost every individual search provides interpretations of their results

in one or even several simplified models that are characteristic of SUSY topologies probed by the analysis.

However, while these models are very convenient for the interpretation of individual SUSY production and decay topologies, care must be taken when applying these limits to more complex SUSY spectra. Therefore, in practice, simplified model limits are often used as an approximation of the constraints that can be placed on sparticle masses in more complex SUSY spectra. Yet, depending on the assumed SUSY spectrum, the sparticle of interest, and the considered simplified model limit, this approximation can lead to a significant mistake, typically an overestimation, in the assumed constraint on the sparticle mass (see for example [67]) . Only on a case-by-case basis can it be determined whether the limit of a given simplified model represents a good approximation of the true underlying constraint that can be applied on a sparticle mass in a complex SUSY spectrum. In the following, we will point out explicitly the assumptions that have entered the limits when quoting interpretations from simplified models.

This review covers results up to September 2017 and since none of the searches performed so far have shown significant excess above the SM background prediction, the interpretation of the presented results are exclusion limits on SUSY parameter space.

113.4. Exclusion limits on gluino and squark masses

Gluinos and squarks are the SUSY partners of gluons and quarks, and thus carry color charge. Limits on squark masses of the order 100 GeV have been set by the LEP experiments [68], in the decay to quark plus neutralino, and for a mass difference between squark and quark plus neutralino of typically at least a few GeV. However, due to the colored production of these particles at hadron colliders (see e.g. Fig. 113.1), hadron collider experiments are able to set much tighter mass limits.

Pair production of these massive colored sparticles at hadron colliders generally involve both the s-channel and t-channel parton-parton interactions. Since there is a negligible amount of bottom and top quark content in the proton, top- and bottom squark production proceeds through s-channel diagrams only. In the past, experimental analyses of squark and/or gluino production typically assumed the first and second generation squarks to be approximately degenerate in mass. However, in order to have even less model dependent interpretations of the searches, the experiments have started to also provide simplified model limits on individual first or second generation squarks.

Assuming R-parity conservation and assuming gluinos to be heavier than squarks, squarks will predominantly decay to a quark and a neutralino or chargino, if kinematically allowed. The decay may involve the lightest neutralino (typically the LSP) or chargino, but, depending on the masses of the gauginos, may involve heavier neutralinos or charginos. For pair production of first and second generation squarks, the simplest decay modes involve two jets and missing momentum, with potential extra jets stemming from initial state or final state radiation (ISR/FSR) or from decay modes with longer cascades. Similarly, gluino pair production leads to four jets and missing momentum, and possibly additional jets from ISR/FSR or cascades. Associated production of a gluino and a (anti-)squark is also possible, in particular if squarks and gluinos have similar masses,

typically leading to three or more jets in the final state. In cascades, isolated photons or leptons may appear from the decays of sparticles such as neutralinos or charginos. Final states are thus characterized by significant missing transverse momentum, and at least two, and possibly many more high p_{T} jets, which can be accompanied by one or more isolated objects like photons or leptons, including τ leptons, in the final state. Table 113.1 shows a schematic overview of characteristic final state signatures of gluino and squark production for different mass hierarchy hypotheses and assuming decays involving the lightest neutralino.

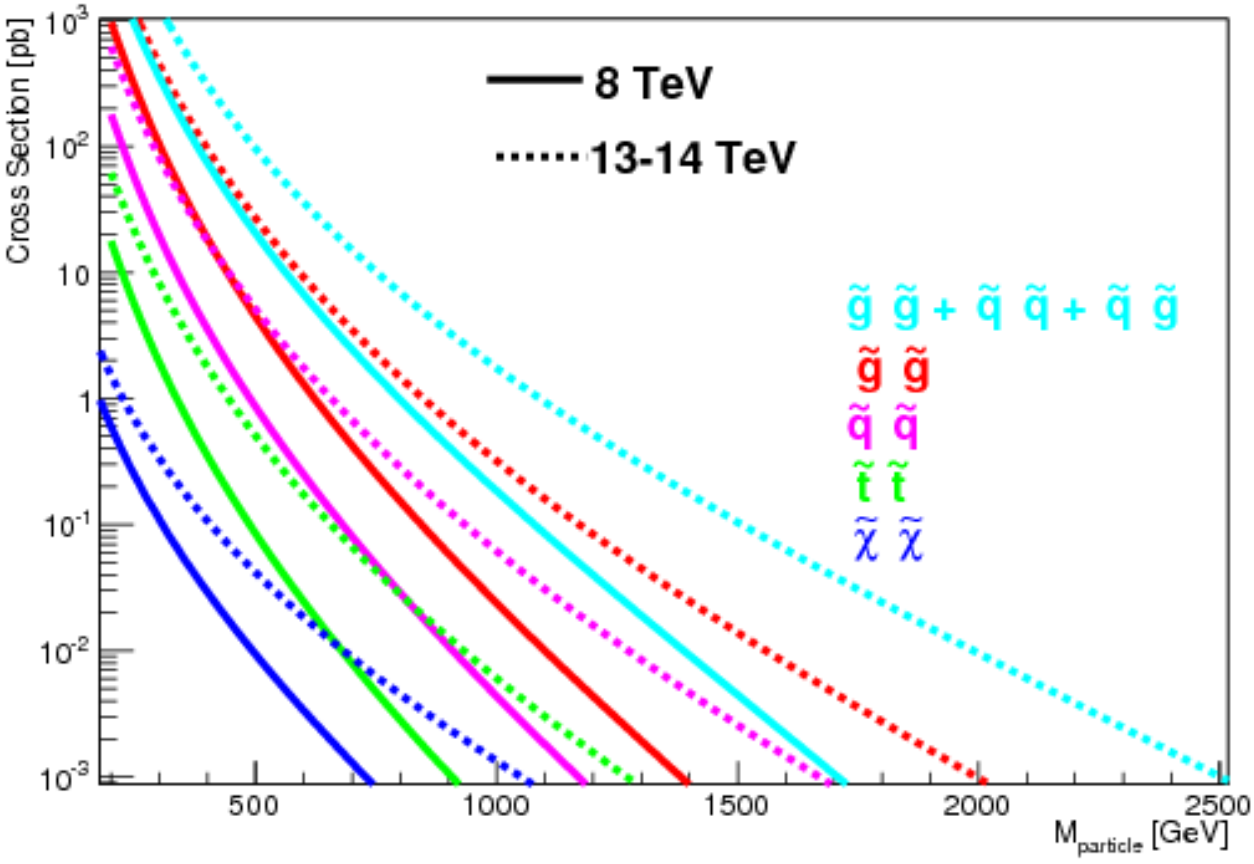

Figure 113.1: Cross sections for pair production of different sparticles as a function of their mass at the LHC for a center-of-mass energy of 8 TeV (solid curves) and 13-14 TeV (dotted curves), taken from Ref. [57]. Typically the production cross section of colored squarks and gluinos, calculated with NLL-FAST [58] at $\sqrt{s}$ =8 and 13 TeV, is several orders of magnitude larger than the one for electroweak gauginos, calculated with PROSPINO [59] at $\sqrt{s}$ =8 and 14 TeV for higgsino-like neutralinos. Except for the explicitly shown pair production of stops, production cross sections for squarks assumes mass degeneracy of left- and right-handed u, d, s, c and b squarks.

Table 113.1: Typical search signatures at hadron colliders for direct gluino and first- and second-generation squark production assuming different mass hierarchies.

Mass Hierarchy	Main Production	Dominant Decay	Typical Signature
$m_{\tilde{q}} \ll m_{\tilde{g}}$	$\tilde{q}\bar{\tilde{q}}, \tilde{q}\tilde{q}$	$\tilde{q} \to q\tilde{\chi}_1^0$	≥ 2 jets + $E_{\mathrm{T}}^{\mathrm{miss}}$ + X
$m_{\tilde{q}} \approx m_{\tilde{g}}$	$\tilde{q}\tilde{g}, \bar{\tilde{q}}\tilde{g}$	$\tilde{q} \to q\tilde{\chi}_1^0$	≥ 3 jets + $E_{\mathrm{T}}^{\mathrm{miss}}$ + X
		$\tilde{g} \to q\bar{q}\tilde{\chi}_1^0$	
$m_{\tilde{q}} \gg m_{\tilde{g}}$	$\tilde{g}\tilde{g}$	$\tilde{g} \to q\bar{q}\tilde{\chi}_1^0$	≥ 4 jets + $E_{\mathrm{T}}^{\mathrm{miss}}$ + X

113.4.1. *Exclusion limits on the gluino mass* :

Limits set by the Tevatron experiments on the gluino mass assume the framework of the CMSSM, with $\tan\beta = 5$ (CDF) or $\tan\beta = 3$ (D0), where $\tan\beta$ is the ratio of vacuum expectation values of the Higgs fields for up-type and down-type fermions. Furthermore, $A_0 = 0$ and $\mu < 0$ is assumed, and the resulting lower mass limits are about 310 GeV for all squark masses, or 390 GeV for the case $m_{\tilde{q}} = m_{\tilde{g}}$ [69,70]. These limits have been superseded by those provided by ATLAS and CMS, and the tightest constraints have been set with up to approximately 36 fb^{-1} of data recorded at the LHC at a center-of-mass energy of 13 TeV.

Limits on the gluino mass have been established in the framework of simplified models. Assuming only gluino pair production, in particular three primary decay chains of the gluino have been considered by the LHC experiments for interpretations of their search results. The first decay chain $\tilde{g} \to q\bar{q}\tilde{\chi}_1^0$ assumes gluino mediated production of first and second generation squarks (on-shell or off-shell) which leads to four light flavor quarks in the final state. Therefore, inclusive all-hadronic analyses searching for multijet plus $E_{\mathrm{T}}^{\mathrm{miss}}$ final states are utilized to put limits on this simplified model. These limits are derived as a function of the gluino and neutralino (LSP) mass. As shown in Fig. 113.2 (upper left), using the cross section from next-to-leading order QCD corrections and the resummation of soft gluon emission at next-to-leading-logarithmic accuracy as reference [58], the ATLAS collaboration [71] excludes in this simplified model gluino masses below approximately 2000 GeV, for a massless neutralino. In scenarios where neutralinos are not very light, the efficiency of the analyses is reduced by the fact that jets are less energetic, and there is less missing transverse momentum in the event. This leads to weaker limits when the mass difference $\Delta m = m_{\tilde{g}} - m_{\tilde{\chi}_1^0}$ is reduced. For example, for neutralino masses above about 1000 GeV no limit on the gluino mass can be set for this decay chain. Therefore, limits on gluino masses are strongly affected by the assumption of the neutralino mass. Similar results for this simplified model have been obtained by CMS [72,73].

The second important decay chain of the gluino considered for interpretation in a simplified model is $\tilde{g} \to b\bar{b}\tilde{\chi}_1^0$. Here the decay is mediated via bottom squarks and thus leads to four jets from b quarks and $E_{\mathrm{T}}^{\mathrm{miss}}$ in the final state. Also for this topology

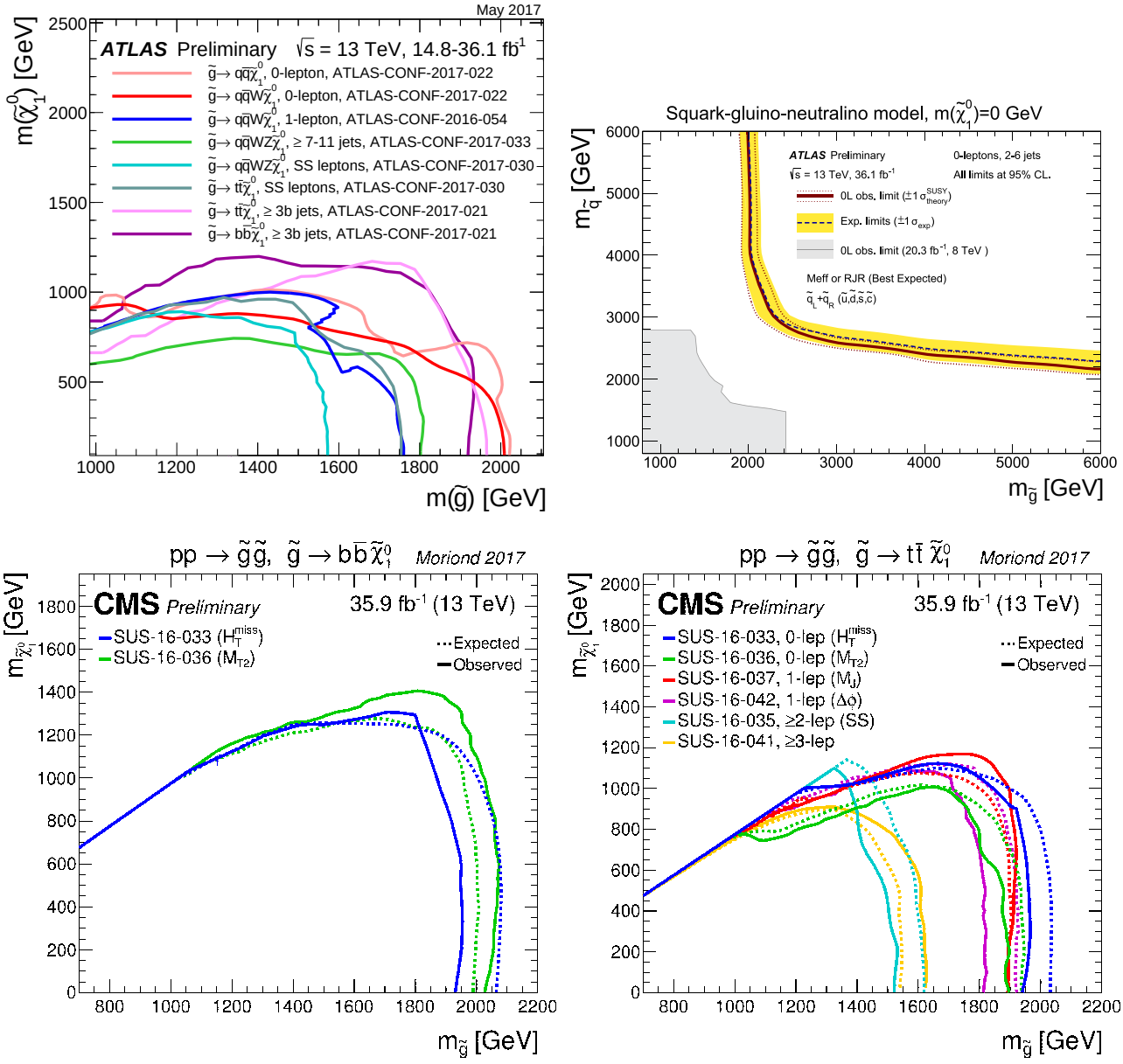

Figure 113.2: Upper left and lower left and right plots: lower mass limits, at 95% C.L., on gluino pair production for various decay chains. The upper left plot shows limits from the ATLAS collaboration; the lower plots display CMS results for the decay chains $\tilde{g} \to b\bar{b}\tilde{\chi}_1^0$ (lower left) and $\tilde{g} \to t\bar{t}\tilde{\chi}_1^0$ (lower right). The limits are defined in the framework of simplified models assuming a single decay chain, i.e. a 100% branching fraction. The upper right plot shows 95% C.L. mass limits on gluinos and squarks assuming gluino and squark production and massless neutralinos.

inclusive all-hadronic searches provide the highest sensitivity. However, with four b quarks in the final state, the use of secondary vertex reconstruction for the identification of jets originating from b quarks provides a powerful handle on the SM background. Therefore,

in addition to a multijet plus $E_{\mathrm{T}}^{\mathrm{miss}}$ signature these searches also require several jets to be tagged as b-jets. As shown in Fig. 113.2 (lower left), for this simplified model CMS [72] excludes gluino masses below ≈ 2000 GeV for a massless neutralino, while for neutralino masses above ≈ 1400 GeV no limit on the gluino mass can be set. Comparable limits for this simplified model are provided by searches from ATLAS [74].

Gluino decays are not limited to first and second generation squarks or bottom squarks, if kinematically allowed, top squarks via the decay $\tilde{g} \to \tilde{t}t$ are also possible. This leads to a "four tops" final state $tttt\tilde{\chi}_1^0\tilde{\chi}_1^0$ and defines the third important simplified model, $\tilde{g} \to t\bar{t}\tilde{\chi}_1^0$, characterizing gluino pair production. The topology of this decay is very rich in different experimental signatures: as many as four isolated leptons, four b-jets, several light flavor quark jets, and significant missing momentum from the neutrinos in the W decay and from the two neutralinos. As shown in Fig. 113.2 (lower right), the CMS inclusive H_{T} based search [73] and a search requiring one isolated lepton and large-radius jets [75] rule out gluinos with masses below ≈ 1900 GeV for massless neutralinos in this model. For neutralino masses above ≈ 1100 GeV, no limit can be placed on the gluino mass. The ATLAS multiple b-jets search [74] obtains similar limits.

The ATLAS collaboration also provides limits in a pMSSM-inspired model with only gluinos and first and second generation squarks, and a bino-like $\tilde{\chi}_1^0$ [71]. As shown in Fig. 113.2 (upper right), assuming $m_{\tilde{\chi}_1^0} = 0$ GeV, gluinos with masses below ≈ 2000 GeV are excluded for any squark mass and vice versa. For $m_{\tilde{q}} \approx m_{\tilde{g}}$, the mass exclusion is about 2700 GeV.

R-parity violating gluino decays are searched for in a number of final states. Searches in multilepton final states set lower mass limits of 1 to 1.4 TeV, depending on neutralino mass and lepton flavor, on decays mediated by λ and λ' couplings [76,77], assuming prompt decays. Searches for displaced vertices are sensitive to non-prompt decays [78]. Multijet final states have been used to search for fully hadronic gluino decays involving λ'', by CDF [79], ATLAS [80,81] and CMS [82,83]. Lower mass limits range between 600 and 2000 GeV depending on neutralino mass and flavor content of the final state.

113.4.2. *Exclusion limits squark masses* :

Limits on first and second generation squark masses set by the Tevatron experiments assume the CMSSM model, and amount to lower limits of about 380 GeV for all gluino masses, or 390 GeV for the case $m_{\tilde{q}} = m_{\tilde{g}}$ [69,70].

At the LHC, limits on squark masses have been set using up to approximately 36 fb^{-1} of data at 13 TeV. Interpretations in simplified models typically characterize squark pair production with only one decay chain of $\tilde{q} \to q\tilde{\chi}_1^0$. Here it is assumed that the left and right-handed $\tilde{u}$, $\tilde{d}$, $\tilde{s}$ and $\tilde{c}$ squarks are degenerate in mass. Furthermore, it is assumed that the mass of the gluino is very high and thus contributions of the corresponding t-channel diagrams to squark pair production are negligible. Therefore, the total production cross section for this simplified model is eight times the production cross section of an individual squark (e.g. $\tilde{u}_L$). The CMS collaboration provides interpretations using different all-hadronic searches for this simplified model. As displayed in the upper plot of Fig. 113.3, best observed exclusion is obtained from the analysis using the m_{T2}

variable [72], which excludes squark masses just below 1550 GeV for a light neutralino. The effects of heavy neutralinos on squark limits are similar to those discussed in the gluino case (see section II.4.1) and only for neutralino masses below ≈ 800 GeV can any squark masses be excluded. Results from the ATLAS collaboration [71] for this simplified model are similar.

For the same analysis ATLAS also provides an interpretation of their search result in the aforementioned pMSSM-inspired model with only gluinos and first and second generation squarks, and a bino-like $\tilde{\chi}_1^0$ [71]. In this model, squark production can take place with non-decoupled gluinos, enhancing the squark production cross section through gluino exchange diagrams. For example, for gluinos of 6 TeV, squark masses up to 2.2 TeV are excluded, much higher than in the simplified model under consideration.

If the assumption of mass degenerate first and second generation squarks is dropped and only the production of a single light squark is assumed, the limits weaken significantly. This is shown as the much smaller exclusion region in the upper plot of Fig. 113.3, which represents the 95% C.L. limit on pair production of a single light squark, with the gluino and all other squarks decoupled to very high masses. Under this assumption, the lower limit on squark masses is only ≈ 1050 GeV for a massless neutralino, and for neutralinos heavier than ≈ 450 GeV no squark mass limit can be placed. It should be noted that this limit is not a result of a simple scaling of the above mentioned mass limits assuming eightfold mass degeneracy but it also takes into account that for an eight times lower production cross section the analyses must probe kinematic regions of phase space that are closer to the ones of SM background production. Since signal acceptance and the ratio of expected signal to SM background events of the analyses are typically worse in this region of phase space not only the 1/8 reduction in production cross section but also a worse analysis sensitivity are responsible for the much weaker limit on single squark pair production.

For single light squarks ATLAS also reports results of a dedicated search, at $\sqrt{s} = 8$ TeV, for pair production of scalar partners of charm quarks [84]. Assuming that the scalar-charm state exclusively decays into a charm quark and a neutralino, scalar-charm masses up to 490 GeV are excluded for neutralino masses below 200 GeV.

Besides placing stringent limits on first and second generation squark masses, the LHC experiments also search for the production of third generation squarks. SUSY at the TeV-scale is often motivated by naturalness arguments, most notably as a solution to stabilize quadratic divergences in radiative corrections to the Higgs boson mass. In this context, the most relevant terms for SUSY phenomenology arise from the interplay between the masses of the third generation squarks and the Yukawa coupling of the top quark to the Higgs boson. This motivates a potential constraint on the masses of the top squarks and the left-handed bottom squark. Due to the large top quark mass, significant mixing between $\tilde{t}_{\mathrm{L}}$ and $\tilde{t}_{\mathrm{R}}$ is expected, leading to a lighter mass state $\tilde{t}_1$ and a heavier mass state $\tilde{t}_2$. In the MSSM, the lightest top squark ($\tilde{t}_1$) can be the lightest squark.

Bottom squarks are expected to decay predominantly to $b\tilde{\chi}^0$ giving rise to the characteristic multi b-jet and $E_{\mathrm{T}}^{\mathrm{miss}}$ signature. Direct production of bottom squark pairs has been studied at the Tevatron and at the LHC. Limits from the Tevatron are

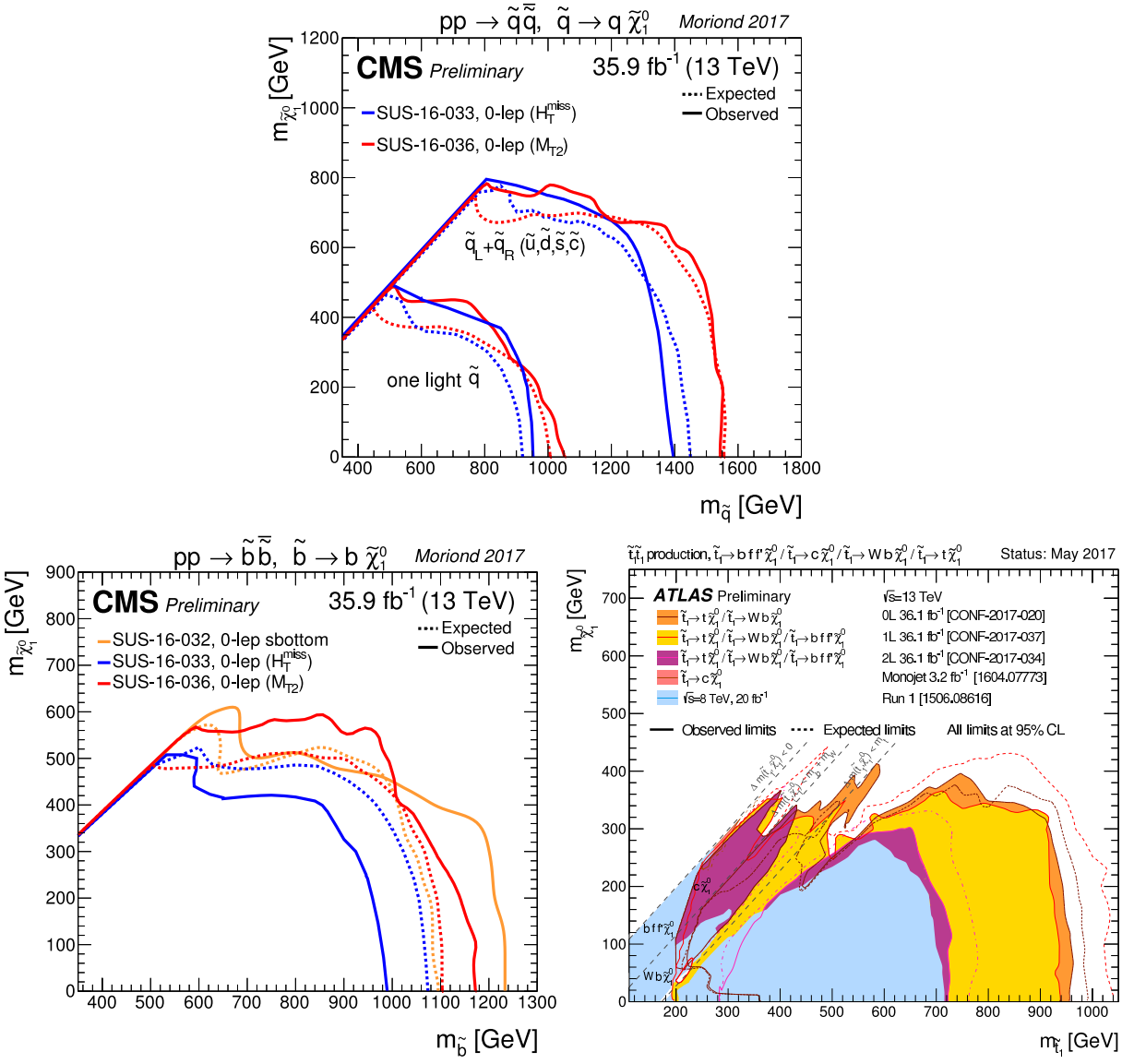

Figure 113.3: The upper plot shows 95% C.L. exclusion contours in the squark-neutralino mass plane defined in the framework of simplified models assuming a single decay chain of $\tilde{q} \to q\tilde{\chi}_1^0$ [72]. Two assumptions for the squark pair production cross sections are displayed; a) eightfold degeneracy for the masses of the first and second generation squarks and b) only one light flavor squark. The lower left plot shows the 95% C.L. exclusion contours in the sbottom-neutralino mass plane defined in the framework of a simplified model assuming a single decay chain of $\tilde{b} \to b\tilde{\chi}_1^0$ as obtained by CMS. The lower right plot shows the 95% C.L. exclusion contours in the stop-neutralino mass plane defined in various simplified models of stop decay, as obtained by ATLAS.

$m_{\tilde{b}} > 247$ GeV for a massless neutralino [85,86]. The LHC experiments have surpassed these limits, and the latest results are based on 36 fb^{-1} of data collected at $\sqrt{s} = 13$ TeV. As shown in the lower left plot of Fig. 113.3, using inclusive all-hadronic searches [72,73] as well as a search requiring significant $E_{\rm T}^{\rm miss}$ and two jets reconstructed as b-jets [87], CMS has set a lower limit of $m_{\tilde{b}} >\approx 1200$ GeV for massless neutralinos in this model. For $m_{\tilde{\chi}_1^0} \approx 550$ GeV or higher no limit can be placed on direct bottom squark pair production in this simplified model. Limits from ATLAS are comparable [88]. Further bottom squark decay modes have also been studied by ATLAS [88,89] and CMS [87,90].

The top squark decay modes depend on the SUSY mass spectrum, and on the $\tilde{t}_{\rm L}$-$\tilde{t}_{\rm R}$ mixture of the top squark mass eigenstate. If kinematically allowed, the two-body decays $\tilde{t} \to t\tilde{\chi}^0$ (which requires $m_{\tilde{t}} - m_{\tilde{\chi}^0} > m_t$) and $\tilde{t} \to b\tilde{\chi}^{\pm}$ (which requires $m_{\tilde{t}} - m_{\tilde{\chi}^{\pm}} > m_b$) are expected to dominate. If not, the top squark decay may proceed either via the two-body decay $\tilde{t} \to c\tilde{\chi}^0$ or through $\tilde{t} \to bf\bar{f}'\tilde{\chi}^0$ (where f and $\bar{f}'$ denote a fermion-antifermion pair with appropriate quantum numbers). For $m_{\tilde{t}} - m_{\tilde{\chi}^0} > m_b$ the latter decay chain represents a four-body decay with a W boson, charged Higgs H, slepton $\tilde{\ell}$, or light flavor squark $\tilde{q}$, exchange. If the exchanged W boson and/or sleptons are kinematically allowed to be on-shell ($m_{\tilde{t}} - m_{\tilde{\chi}^{\pm}} > m_b + m_W$ and/or $m_{\tilde{t}} - m_{\tilde{\ell}} > m_b$), the three-body decays $\tilde{t} \to Wb\tilde{\chi}^0$ and/or $\tilde{t} \to bl\tilde{\ell}$ will become dominant. For further discussion on top squark decays see for example Ref. [91].

Limits from LEP on the $\tilde{t}_1$ mass are $m_{\tilde{t}} > 96$ GeV in the charm plus neutralino final state, and > 93 GeV in the lepton, b-quark and sneutrino final state [68].

The Tevatron experiments have performed a number of searches for top squarks, often assuming direct pair production. In the $b\ell\tilde{\nu}$ decay channel, and assuming a 100% branching fraction, limits are set as $m_{\tilde{t}} > 210$ GeV for $m_{\tilde{\nu}} < 110$ GeV and $m_{\tilde{t}} - m_{\tilde{\nu}} > 30$ GeV, or $m_{\tilde{t}} > 235$ GeV for $m_{\tilde{\nu}} < 50$ GeV [92,93]. In the $\tilde{t} \to c\tilde{\chi}^0$ decay mode, a top squark with a mass below 180 GeV is excluded for a neutralino lighter than 95 GeV [94,95]. In both analyses, no limits on the top squark can be set for heavy sneutrinos or neutralinos. In the $\tilde{t} \to b\tilde{\chi}_1^{\pm}$ decay channel, searches for a relatively light top squark have been performed in the dilepton final state [96,97]. The CDF experiment sets limits in the $\tilde{t} - \tilde{\chi}_1^0$ mass plane for various branching fractions of the chargino decay to leptons and for two value of $m_{\tilde{\chi}_1^{\pm}}$. For $m_{\tilde{\chi}_1^{\pm}} = 105.8$ GeV and $m_{\tilde{\chi}_1^0} = 47.6$ GeV, top squarks between 128 and 135 GeV are excluded for W-like leptonic branching fractions of the chargino.

The LHC experiments have improved these limits substantially. As shown in the right plot of Fig. 113.3, limits on the top squark mass assuming a simplified model with a single decay chain of $\tilde{t} \to t\tilde{\chi}_1^0$ now approach or surpass 1 TeV. The most important searches for this top squark decay topology are dedicated searches requiring zero or one isolated lepton, modest $E_{\rm T}^{\rm miss}$, and four or more jets out of which at least one jet must be reconstructed as a b-jet [98–101]. For example, CMS excludes top squarks with masses below about 1100 GeV in this model for massless neutralinos, while for $m_{\tilde{\chi}_1^0} >$ 500 GeV no limits can be provided.

Assuming that the top squark decay exclusively proceeds via the chargino mediated

decay chain $\tilde{t} \to b\tilde{\chi}_1^{\pm}$, $\tilde{\chi}_1^{\pm} \to W^{\pm(*)}\tilde{\chi}_1^0$ yields stop mass exclusion limits that vary strongly with the assumptions made on the $\tilde{t} - \tilde{\chi}_1^{\pm} - \tilde{\chi}_1^0$ mass hierarchy. For example, for $m_{\tilde{\chi}_1^{\pm}} = (m_{\tilde{t}} + m_{\tilde{\chi}_1^0})/2$, a stop mass below ≈ 1000 GeV for a light $\tilde{\chi}_1^0$ is excluded, while no limit can be placed for $m_{\tilde{\chi}_1^0} > 500$ GeV [98]. These limits, however, can weaken significantly when other assumptions about the mass hierarchy are imposed. For example, if the chargino becomes nearly mass degenerate with the top squark the key experimental signature turns from an all-hadronic final state with b-jets and $E_{\mathrm{T}}^{\mathrm{miss}}$ into a multi-lepton and $E_{\mathrm{T}}^{\mathrm{miss}}$ topology yielding typically weaker limits for this top squark decay (see e.g. [99,101,102]) .

If the decays $\tilde{t} \to t\tilde{\chi}_1^0$ and $\tilde{t} \to b\tilde{\chi}_1^{\pm}$, $\tilde{\chi}_1^{\pm} \to W^{\pm(*)}\tilde{\chi}_1^0$ are kinematically forbidden, the decay chains $\tilde{t} \to Wb\tilde{\chi}^0$ and $\tilde{t} \to c\tilde{\chi}^0$ can become important. As shown in the lower right plot of Fig. 113.3, the zero-lepton ATLAS search provides for the kinematic region $m_{\tilde{t}} - m_{\tilde{\chi}^{\pm}} > m_b + m_W$ lower limits on the top squark mass of ≈ 400 GeV for a neutralino lighter than ≈ 300 GeV [100], while the corresponding CMS analyses [72,73,98] push this limit to about 550 GeV for neutralino masses below ≈ 400 GeV. Furthermore, analyses with one or two lepton final states [99,101–103] also place significant constraints on this decay channel.

For the kinematic region in which even the production of real W bosons is not allowed, ATLAS and CMS improve the Tevatron limit on $\tilde{t} \to c\tilde{\chi}^0$ substantially. Based on a monojet analysis [104] ATLAS excludes top squark masses below $m_{\tilde{\chi}_1^0} \approx 450$ GeV along the kinematic boundary for the $\tilde{t} \to c\tilde{\chi}^0$ decay. The CMS collaboration uses the hadronic searches [72,98] to place constraints on this particular stop decay and excludes $m_{\tilde{t}} \approx 550$ GeV for $m_{\tilde{\chi}_1^0}$ below 450 GeV. The exclusion at the diagonal $m_{\tilde{t}} \approx m_{\tilde{\chi}_1^0}$ is also about 550 GeV.

The other decay chain relevant in this phase region is $\tilde{t} \to bf\bar{f}'\tilde{\chi}^0$. Here the ATLAS one-lepton search [101] excludes up to $m_{\tilde{t}} \approx 350$ GeV for $m_{\tilde{\chi}_1^0}$ below 250 GeV, while the monojet analysis [104] excludes at the kinematic boundary top squarks below 400 GeV. As for the $\tilde{t} \to c\tilde{\chi}^0$ decay, CMS uses the zero-lepton searches [72,98] to also place constraints on $\tilde{t} \to bf\bar{f}'\tilde{\chi}^0$. Also in this case CMS excludes $m_{\tilde{t}} \approx 550$ GeV for $m_{\tilde{\chi}_1^0}$ below 450 GeV.

In general, the variety of top squark decay chains in the phase space region where $\tilde{t} \to t\tilde{\chi}_1^0$ is kinematically forbidden represents a challenge for the experimental search program and more data and refined analyses will be required to further improve the sensitivity in this difficult but important region of SUSY parameter space.

R-parity violating production of single squarks via a λ'-type coupling has been studied at HERA. In such models, a lower limit on the squark mass of the order of 275 GeV has been set for electromagnetic-strength-like couplings $\lambda' = 0.3$ [105]. At the LHC, both prompt [76,77] and non-prompt [78,106] R-parity violating squark decays have been searched for, but no signal was found. Squark mass limits are very model-dependent.

R-parity violating production of single top squarks has been searched for at LEP, HERA, and the Tevatron. For example, an analysis from the ZEUS collaboration [107]

makes an interpretation of its search result assuming top squarks to be produced via a λ' coupling and decay either to $b\tilde{\chi}_1^{\pm}$ or R-parity-violating to a lepton and a jet. Limits are set on λ'_{131} as a function of the top squark mass in an MSSM framework with gaugino mass unification at the GUT scale.

The search for top squark pair production in the context of R-parity violating supersymmetry has now also become a focus point for searches at the LHC. The CMS collaboration has performed a search for top squarks using a variety of multilepton final states [108]. It provides lower limits on the top squark mass in models with non-zero leptonic R-parity violating couplings λ_{122} and λ_{233}. For a bino mass of 200 GeV, these limits are 1020 GeV and 820 GeV, respectively. The analysis also provides limits in a model with the semileptonic R-parity violating coupling λ'_{233}. The λ'-mediated top squark decay $\tilde{t} \to b\ell$ has been studied by ATLAS for prompt decays [109], and by CMS for non-prompt decays [110]. CMS also searched for the λ'-mediated decay $\tilde{t} \to b\ell qq$, setting lower stop mass limits of 890 GeV (e) or 1000 GeV (μ) [111]. The fully hadronic R-parity violating top squark decays $\tilde{t} \to bs$ and $\tilde{t} \to ds$, involving λ'', have been searched for by ATLAS [112], and lower top squark mass limits between 410 and 610 GeV were set. CMS [113] have searched for a top squark decay to a bottom quark and a light-flavor quark, and excludes top squarks with masses between 200 and 385 GeV in this decay mode.

It should be noted that limits discussed in this section belong to different top and bottom squark decay channels, different sparticle mass hierarchies, and different simplified decay scenarios. Therefore, care must be taken when interpreting these limits in the context of more complete SUSY models.

113.4.3. *Summary of exclusion limits on squarks and gluinos assuming R-Parity conservation* :

A summary of the most important squark and gluino mass limits for different interpretation approaches assuming R-parity conservation is shown in Table 113.2.

For gluino masses rather similar limits of about 2 TeV are obtained from different model assumptions, indicating that the LHC is indeed probing direct gluino production at the TeV scale and beyond. However, for neutralino masses above approximately 1 to 1.4 TeV, in the best case scenarios, ATLAS and CMS searches cannot place any limits on the gluino mass.

Limits on direct squark production, on the other hand, depend strongly on the chosen model. Especially for direct production of top squarks there are still large regions in parameter space where masses below 1 TeV cannot be excluded. This is also true for first and second generation squarks when only one single squark is considered. Furthermore, for neutralino masses above ≈ 500 GeV no limit on any direct squark production scenario can be placed by the LHC.

Table 113.2: Summary of squark mass and gluino mass limits using different interpretation approaches assuming R-parity conservation. Masses in this table are provided in GeV. Further details about assumption and analyses from which these limits are obtained are discussed in the corresponding sections of the text.

Model	Assumption	$m_{\tilde{q}}$	$m_{\tilde{g}}$
Simplified model	$m_{\tilde{\chi}_1^0}$= 0, $m_{\tilde{q}} \approx m_{\tilde{g}}$	$\approx$ 2700	$\approx$ 2700
$\tilde{g}\tilde{q}, \tilde{g}\bar{\tilde{q}}$	$m_{\tilde{\chi}_1^0}$= 0, all $m_{\tilde{q}}$	-	$\approx$ 2000
p	$m_{\tilde{\chi}_1^0}$= 0, all $m_{\tilde{g}}$	$\approx$ 2000	-
Simplified models $\tilde{g}\tilde{g}$			
$\tilde{g} \to q\bar{q}\tilde{\chi}_1^0$	$m_{\tilde{\chi}_1^0}$ =0	-	$\approx$ 2000
	$m_{\tilde{\chi}_1^0} > \approx$ 1000	-	no limit
$\tilde{g} \to b\bar{b}\tilde{\chi}_1^0$	$m_{\tilde{\chi}_1^0}$ =0	-	$\approx$ 2000
	$m_{\tilde{\chi}_1^0} > \approx$ 1400	-	no limit
$\tilde{g} \to t\bar{t}\tilde{\chi}_1^0$	$m_{\tilde{\chi}_1^0}$ =0	-	$\approx$ 1900
	$m_{\tilde{\chi}_1^0} > \approx$ 1100	-	no limit
Simplified models $\tilde{q}\tilde{q}$			
$\tilde{q} \to q\tilde{\chi}_1^0$	$m_{\tilde{\chi}_1^0}$ =0	$\approx$ 1550	-
	$m_{\tilde{\chi}_1^0} > \approx$ 800	no limit	-
$\tilde{u}_L \to q\tilde{\chi}_1^0$	$m_{\tilde{\chi}_1^0}$ =0	$\approx$ 1050	-
	$m_{\tilde{\chi}_1^0} > \approx$ 450	no limit	-
$\tilde{b} \to b\tilde{\chi}_1^0$	$m_{\tilde{\chi}_1^0}$ =0	$\approx$ 1200	-
	$m_{\tilde{\chi}_1^0} > \approx$ 550	no limit	-
$\tilde{t} \to t\tilde{\chi}_1^0$	$m_{\tilde{\chi}_1^0}$ =0	$\approx$ 1100	-
	$m_{\tilde{\chi}_1^0} > \approx$ 500	no limit	-
$\tilde{t} \to b\tilde{\chi}_1^{\pm}$	$m_{\tilde{\chi}_1^0}$ =0	$\approx$ 1000	-
$[m_{\tilde{\chi}_1^{\pm}} = (m_{\tilde{t}} - m_{\tilde{\chi}_1^0})/2]$	$m_{\tilde{\chi}_1^0} > \approx$ 500	no limit	-
$\tilde{t} \to Wb\tilde{\chi}_1^0$	$m_{\tilde{\chi}_1^0} < \approx$ 400	$\approx$ 550	-
$[m_W < m_{\tilde{t}} - m_{\tilde{\chi}^0} < m_t]$			
$\tilde{t} \to c\tilde{\chi}_1^0$	$m_{\tilde{\chi}_1^0} < \approx$ 450	$\approx$ 550	-
	$m_{\tilde{t}} \approx m_{\tilde{\chi}_1^0}$	$\approx$ 550	-
$\tilde{t} \to bff'\tilde{\chi}_1^0$	$m_{\tilde{\chi}_1^0} < \approx$ 450	$\approx$ 550	-
	$m_{\tilde{t}} \approx m_{\tilde{\chi}_1^0}$	$\approx$ 550	-
$[m_{\tilde{t}} - m_{\tilde{\chi}^0} < m_W]$			

113.5. Exclusion limits on the masses of charginos and neutralinos

Charginos and neutralinos result from mixing of the charged wino and higgsino states, and the neutral bino, wino and higgsino states, respectively. The mixing is determined by a limited number of parameters. For charginos these are the wino mass parameter M_2, the higgsino mass parameter μ, and $\tan\beta$, and for neutralinos these are the same parameters plus the bino mass parameter M_1. If any of the parameters M_1, M_2 or μ happened to be substantially smaller than the others, the chargino and neutralino composition would be dominated by specific states, which are referred to as bino-like ($M_1 \ll M_2, \mu$), wino-like ($M_2 \ll M_1, \mu$), or higgsino-like ($\mu \ll M_1, M_2$). If gaugino mass unification at the GUT scale is assumed, a relation between M_1 and M_2 at the electroweak scale follows: $M_1 = 5/3 \tan^2\theta_W M_2 \approx 0.5 M_2$, with θ_W the weak mixing angle. Charginos and neutralinos carry no color charge.

113.5.1. *Exclusion limits on chargino masses* :

If kinematically allowed, two body decay modes such as $\tilde{\chi}^{\pm} \to \tilde{f}\bar{f}'$ (including $\ell\tilde{\nu}$ and $\tilde{\ell}\nu$) are dominant. If not, three body decay $\tilde{\chi}^{\pm} \to f\bar{f}'\tilde{\chi}^0$ are mediated through virtual W bosons or sfermions. If sfermions are heavy, the W mediation dominates, and $f\bar{f}'$ are distributed with branching fractions similar to W decay products (barring phase space effects for small mass gaps between $\tilde{\chi}^{\pm}$ and $\tilde{\chi}^0$). If, on the other hand, sleptons are light enough to play a significant role in the decay mediation, leptonic final states will be enhanced.

At LEP, charginos have been searched for in fully-hadronic, semi-leptonic and fully leptonic decay modes [114,115]. A general lower limit on the lightest chargino mass of 103.5 GeV is derived, except in corners of phase space with low electron sneutrino mass, where destructive interference in chargino production, or two-body decay modes, play a role. The limit is also affected if the mass difference between $\tilde{\chi}_1^{\pm}$ and $\tilde{\chi}_1^0$ is small; dedicated searches for such scenarios set a lower limit of 92 GeV.

At the Tevatron, charginos have been searched for via associated production of $\tilde{\chi}_1^{\pm}\tilde{\chi}_2^0$ [116,117]. Decay modes involving multilepton final states provide the best discrimination against the large multijet background. Analyses have looked for at least three charged isolated leptons, for two leptons with missing transverse momentum, or for two leptons with the same charge. Depending on the $(\tilde{\chi}_1^{\pm} - \tilde{\chi}_1^0)$ and/or $(\tilde{\chi}_2^0 - \tilde{\chi}_1^0)$ mass differences, leptons may be soft.

At the LHC, the search strategy is similar to that at the Tevatron. As shown in Fig. 113.1, the cross section of pair production of electroweak gauginos at the LHC, for masses of several hundreds of GeV, is at least two orders of magnitude smaller than for colored SUSY particles (e.g. top squark pair production). For this reason a high statistics data sample is required to improve the sensitivity of LEP and Tevatron searches for direct chargino/neutralino production. With the full LHC Run 1 data and the first set of Run 2 data, ATLAS and CMS have started to surpass the limits from LEP and Tevatron in regions of SUSY parameter space.

Chargino pair production is searched for in the dilepton plus missing momentum final state. In the simplified model interpretation of the results, assuming mediation of the chargino decay by light sleptons, ATLAS [118] sets limits on the chargino mass up to

740 GeV for massless LSPs, but no limits on the chargino mass can be set for $\tilde{\chi}_1^0$ heavier than 350 GeV. Limits are fairly robust against variation of the slepton mass, unless the mass gap between chargino and slepton becomes small. At 8 TeV, first limits were also set on charginos decaying via a W boson [119]: chargino masses below 180 GeV are excluded for massless LSPs, but no limits are set for LSPs heavier than 25 GeV.

The trilepton plus missing momentum final state is used to set limits on $\tilde{\chi}_1^\pm \tilde{\chi}_2^0$ production, assuming wino-like $\tilde{\chi}^\pm$ and $\tilde{\chi}_2^0$, bino-like $\tilde{\chi}_1^0$, and $m_{\tilde{\chi}^\pm} = m_{\tilde{\chi}_2^0}$, leaving $m_{\tilde{\chi}^\pm}$ and $m_{\tilde{\chi}_1^0}$ free. Again, the branching fraction of leptonic final states is determined by the slepton masses. If the decay is predominantly mediated by a light $\tilde{\ell}_\mathrm{L}$, i.e. $\tilde{\ell}_\mathrm{R}$ is assumed to be heavy, the three lepton flavors will be produced in equal amounts. It is assumed that $\tilde{\ell}_\mathrm{L}$ and sneutrino masses are equal, and diagrams with sneutrinos are included. In this scenario, ATLAS [118] and CMS [120] exclude chargino masses below 1140 GeV for massless LSPs; no limits are set for LSP masses above 700 GeV. If the decay is dominated by a light $\tilde{\ell}_\mathrm{R}$, the chargino cannot be a pure wino but needs to have a large higgsino component, preferring the decays to tau leptons. Limits are set in various scenarios. If, like for $\tilde{\ell}_\mathrm{L}$, a flavor-democratic scenario is assumed, CMS sets limits of 1060 GeV on the chargino mass for massless LSPs, but under the assumption that both $\tilde{\chi}^\pm$ and $\tilde{\chi}_2^0$ decay leads to tau leptons in the final state, the chargino mass limit deteriorates to 620 GeV for massless LSPs [120]. ATLAS assumes a simplified model in which staus are significantly lighter than the other sleptons in order to search for a similar multi-tau final state, and sets a lower limit on the chargino mass of 760 GeV in this model [121].

If sleptons are heavy, the chargino is assumed to decay to a W boson plus LSP, and the $\tilde{\chi}_2^0$ into Z plus LSP or H plus LSP. In the WZ channel, ATLAS [118] and CMS [122] limits on the chargino mass reach 610 GeV for massless LSPs, but no limits are set for LSPs heavier than 250 GeV. In the WH channel, for $m_H = 125$ GeV and using Higgs decays to $b\bar{b}$, $\gamma\gamma$ and WW (ATLAS [123]) , or Higgs decays to $b\bar{b}$, $\gamma\gamma$, WW, ZZ and $\tau^+\tau^-$ (CMS [122]) , assuming a SM-like branching fraction in these final states, chargino mass limits extend up to 480 GeV for massless LSPs, but vanish for LSP masses above 100 GeV.

The results on electroweak gaugino searches interpreted in simplified models are summarized in Fig. 113.4 for the two cases of light or decoupled sleptons. For both cases, ATLAS and CMS have comparable limits.

In both the wino region (a characteristic of anomaly-mediated SUSY breaking models) and the higgsino region of the MSSM, the mass splitting between $\tilde{\chi}_1^\pm$ and $\tilde{\chi}_1^0$ is small. The chargino decay products are very soft and may escape detection. These compressed spectra are very hard to find, and have triggered dedicated search strategies, which, however, still have limited sensitivity. Photons or jets from initial state radiation may be used to tag such decays. An alternative production mode of electroweak gauginos is provided by vector-boson-fusion, where two additional jets with a large rapidity gap can be used to select events and suppress backgrounds [124,125].

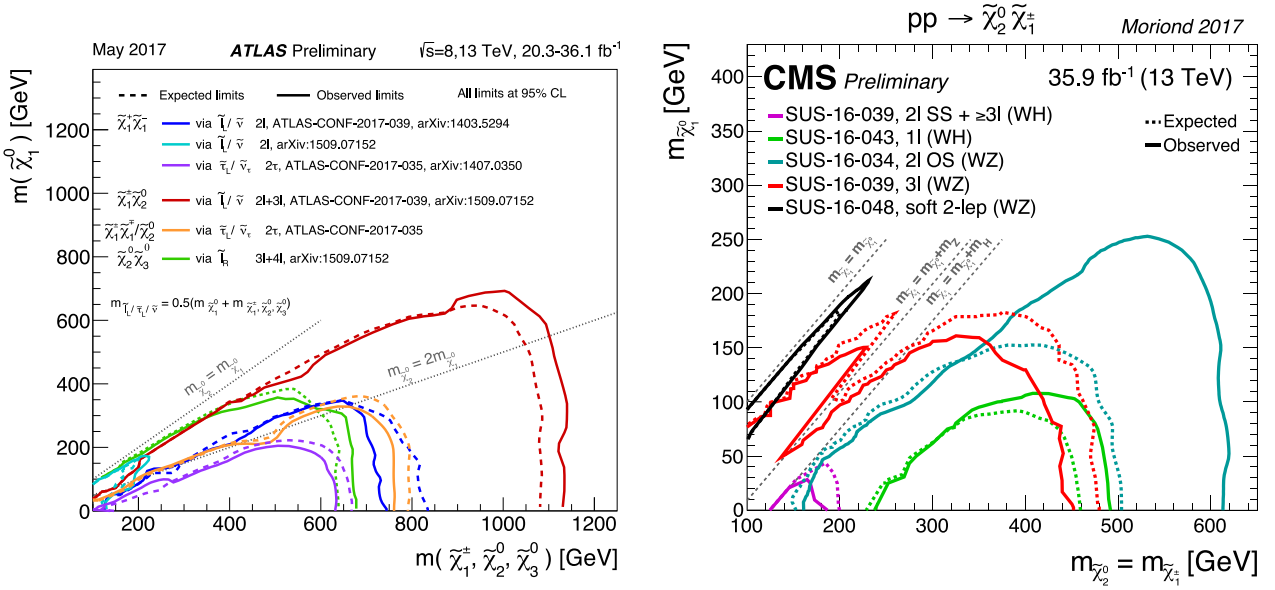

Figure 113.4: LHC exclusion limits on chargino and neutralino masses in a number of simplified models. Left: limits on chargino and neutralino masses for pair production of charginos, pair production of heavier neutralinos, or pair production of chargino and neutralino, under the assumption of light sleptons mediating the decays. Right: limits on chargino and neutralino masses for pair production of chargino and neutralino, under the assumption of decoupled sleptons, and chargino/neutralino decay through W^*, Z^* or H.

113.5.2. *Exclusion limits on neutralino masses* :

In a considerable part of the MSSM parameter space, and in particular when demanding that the LSP carries no electric or color charge, the lightest neutralino $\tilde{\chi}_1^0$ is the LSP. If R-parity is conserved, such a $\tilde{\chi}_1^0$ is stable. Since it is weakly interacting, it will typically escape detectors unseen. Limits on the invisible width of the Z boson apply to neutralinos with a mass below 45.5 GeV, but depend on the Z-neutralino coupling. Such a coupling could be small or even absent; in such a scenario there is no general lower limit on the mass of the lightest neutralino [126]. In models with gaugino mass unification and sfermion mass unification at the GUT scale, a lower limit on the neutralino mass is derived from limits from direct searches, notably for charginos and sleptons, and amounts to 47 GeV [127]. Assuming a constraining model like the CMSSM, this limit increases to 50 GeV at LEP; however the strong constraints now set by the LHC increase such CMSSM-derived $\tilde{\chi}_1^0$ mass limits to well above 200 GeV [128].

In gauge-mediated SUSY breaking models (GMSB), the LSP is typically a gravitino, and the phenomenology is determined by the nature of the next-to-lightest supersymmetric particle (NLSP). A NLSP neutralino will decay to a gravitino and a SM particle whose nature is determined by the neutralino composition. Final states with two high p_T photons and missing momentum are searched for, and interpreted in gauge mediation models with bino-like neutralinos [129–133].

Assuming the production of at least two neutralinos per event, neutralinos with large non-bino components can also be searched for by their decay in final states with missing momentum plus any two bosons out of the collection γ, Z, H. A number of searches at the LHC have tried to cover the rich phenomenology of the various Z and H decay modes [120,132–135].

Heavier neutralinos, in particular $\tilde{\chi}_2^0$, have been searched for in their decays to the lightest neutralino plus a γ, a Z boson or a Higgs boson. Limits on electroweak production of $\tilde{\chi}_2^0$ plus $\tilde{\chi}_1^\pm$ from trilepton analyses have been discussed in the section on charginos; the assumption of equal mass of $\tilde{\chi}_2^0$ and $\tilde{\chi}_1^\pm$ make the limits on chargino masses apply to $\tilde{\chi}_2^0$ as well. Multilepton analyses have also been used to set limits on $\tilde{\chi}_2^0\tilde{\chi}_3^0$ production; assuming equal mass and decay through light sleptons, limits are set up to 680 GeV for massless LSPs [124]. Again, compressed spectra with small mass differences between the heavier neutralinos and the LSP form the most challenging region.

In $\tilde{\chi}_2^0$ decays to $\tilde{\chi}_1^0$ and a lepton pair, the lepton pair invariant mass distribution may show a structure that can be used to measure the $\tilde{\chi}_2^0 - \tilde{\chi}_1^0$ mass difference in case of a signal [36]. This structure, however, can also be used in the search strategy itself, as demonstrated by ATLAS [134] and CMS [136].

In models with R-parity violation, the lightest neutralino can decay even if it is the lightest supersymmetric particle. If the decay involves a non-zero λ coupling, the final state will be a multi-lepton one. Searches for events with four or more isolated charged leptons by ATLAS [76,137] and CMS [77] are interpreted in such models. With very small coupling values, the neutralino would be long-lived, leading to lepton pairs with a displaced vertex, which have also been searched for [78,106].

Searches for events with a displaced hadronic vertex, with or without a matched lepton, are interpreted in a model with R-parity violating neutralino decay involving a non-zero λ' coupling [78,138]. Neutralino decays involving non-zero λ'' lead to fully hadronic final states, and searches for jet-pair resonances are used to set limits, typically on the production of colored particles like top squarks or gluinos, which are assumed to be the primary produced sparticles in these interpretations, as discussed earlier.

The limits on weak gauginos in simplified models are summarized in Table 113.3. Interpretations of the search results outside simplified models, such as in the phenomenological MSSM [139–141], show that the simplified model limits must be interpreted with care. Electroweak gauginos in models that are compatible with the relic density of dark matter in the universe, for example, have particularly tuned mixing parameters and mass spectra, which are not always captured by the simplified models used.

Table 113.3: Summary of weak gaugino mass limits in simplified models, assuming R-parity conservation. Masses in the table are provided in GeV. Further details about assumptions and analyses from which these limits are obtained are discussed in the text.

Assumption	m_χ
$\tilde{\chi}_1^\pm$, all $\Delta m(\tilde{\chi}_1^\pm, \tilde{\chi}_1^0)$	> 92
$\tilde{\chi}_1^\pm$ $\Delta m > 5$, $m_{\tilde{\nu}} > 300$	> 103.5
$\tilde{\chi}_1^\pm$, $m_{(\tilde{\ell},\tilde{\nu})} = (m_{\tilde{\chi}_1^\pm} + m_{\tilde{\chi}_1^0})/2$	
$m_{\tilde{\chi}_1^0} \approx 0$	> 740
$\tilde{\chi}_1^\pm$, $m_{\tilde{\chi}_1^0} > 350$	no LHC limit
$\tilde{\chi}_1^\pm$, $m_{\tilde{\ell}} > m_{\tilde{\chi}_1^\pm}$	
$m_{\tilde{\chi}_1^0} \approx 0$	> 180
$\tilde{\chi}_1^\pm$, $m_{\tilde{\chi}_1^0} > 25$	no LHC limit
$m_{\tilde{\chi}_1^\pm} = m_{\tilde{\chi}_2^0}$, $m_{\tilde{\ell}_\mathrm{L}} = (m_{\tilde{\chi}_1^\pm} + m_{\tilde{\chi}_1^0})/2$	
$m_{\tilde{\chi}_1^0} \approx 0$	> 1140
$m_{\tilde{\chi}_1^0} > 700$	no LHC limit
$m_{\tilde{\chi}_1^\pm} = m_{\tilde{\chi}_2^0}$, $m_{\tilde{\ell}_\mathrm{R}} = (m_{\tilde{\chi}_1^\pm} + m_{\tilde{\chi}_1^0})/2$	flavor-democratic
$m_{\tilde{\chi}_1^0} \approx 0$	> 1060
$m_{\tilde{\chi}_1^0} > 600$	no LHC limit
$m_{\tilde{\chi}_1^\pm} = m_{\tilde{\chi}_2^0}$, $m_{\tilde{\tau}} = (m_{\tilde{\chi}_1^\pm} + m_{\tilde{\chi}_1^0})/2$	$\tilde{\tau}$-dominated
$m_{\tilde{\chi}_1^0} \approx 0$	> 620
$m_{\tilde{\chi}_1^0} > 260$	no LHC limit
$m_{\tilde{\chi}_1^\pm} = m_{\tilde{\chi}_2^0}$, $m_{\tilde{\ell}} > m_{\tilde{\chi}_1^\pm}$, $\mathrm{BF}(WZ) = 1$	
$m_{\tilde{\chi}_1^0} \approx 0$	> 610
$m_{\tilde{\chi}_1^0} > 250$	no LHC limit
$m_{\tilde{\chi}_1^\pm} = m_{\tilde{\chi}_2^0}$, $m_{\tilde{\ell}} > m_{\tilde{\chi}_1^\pm}$, $\mathrm{BF}(WH) = 1$	
$m_{\tilde{\chi}_1^0} \approx 0$	> 480
$m_{\tilde{\chi}_1^0} > 100$	no LHC limit

113.6. Exclusion limits on slepton masses

In models with slepton and gaugino mass unification at the GUT scale, the right-handed slepton, $\tilde{\ell}_\mathrm{R}$, is expected to be lighter than the left-handed slepton, $\tilde{\ell}_\mathrm{L}$. For tau sleptons there may be considerable mixing between the L and R states, leading to a significant mass difference between the lighter $\tilde{\tau}_1$ and the heavier $\tilde{\tau}_2$.

113.6.1. ***Exclusion limits on the masses of charged sleptons*** :

The most model-independent searches for selectrons, smuons and staus originate from the LEP experiments [142]. Smuon production only takes place via s-channel γ^*/Z exchange. Search results are often quoted for $\tilde{\mu}_R$, since it is typically lighter than $\tilde{\mu}_L$ and has a weaker coupling to the Z boson; limits are therefore conservative. Decays are expected to be dominated by $\tilde{\mu}_R \to \mu\tilde{\chi}_1^0$, leading to two non-back-to-back muons and missing momentum. Slepton mass limits are calculated in the MSSM under the assumption of gaugino mass unification at the GUT scale, and depend on the mass difference between the smuon and $\tilde{\chi}_1^0$. A $\tilde{\mu}_R$ with a mass below 94 GeV is excluded for $m_{\tilde{\mu}_R} - m_{\tilde{\chi}_1^0} > 10$ GeV. The selectron case is similar to the smuon case, except that an additional production mechanism is provided by t-channel neutralino exchange. The $\tilde{e}_R$ lower mass limit is 100 GeV for $m_{\tilde{\chi}_1^0} < 85$ GeV. Due to the t-channel neutralino exchange, $\tilde{e}_R\tilde{e}_L$ pair production was possible at LEP, and a lower limit of 73 GeV was set on the selectron mass regardless of the neutralino mass by scanning over MSSM parameter space [143]. The potentially large mixing between $\tilde{\tau}_L$ and $\tilde{\tau}_R$ not only makes the $\tilde{\tau}_1$ light, but can also make its coupling to the Z boson small. LEP lower limits on the $\tilde{\tau}$ mass range between 87 and 93 GeV depending on the $\tilde{\chi}_1^0$ mass, for $m_{\tilde{\tau}} - m_{\tilde{\chi}_1^0} > 7$ GeV [142].

At the LHC, pair production of sleptons is not only heavily suppressed with respect to pair production of colored SUSY particles but the cross section is also almost two orders of magnitude smaller than the one of pair production of charginos and neutralinos. Only with the full Run 1 LHC data set and the first data of Run 2, ATLAS and CMS have started to surpass the sensitivity of the LEP analyses under certain assumptions.

ATLAS and CMS have searched for direct production of selectron pairs and smuon pairs at the LHC, with each slepton decaying to its corresponding SM partner lepton and the $\tilde{\chi}_1^0$ LSP. In simplified models, ATLAS [118] and CMS [120] set lower mass limits on sleptons of 500 GeV for degenerate $\tilde{\ell}_L$ and $\tilde{\ell}_R$, for a massless $\tilde{\chi}_1^0$ and assuming equal selectron and smuon masses, as shown in Fig. 113.5. The limits deteriorate with increasing $\tilde{\chi}_1^0$ mass due to decreasing missing momentum and lepton momentum. As a consequence, no limits are set for $\tilde{\chi}_1^0$ masses above 270 GeV.

In gauge-mediated SUSY breaking models, sleptons can be (co-)NLSPs, *i.e.*, the next-to-lightest SUSY particles and almost degenerate in mass, decaying to a lepton and a gravitino. This decay can either be prompt, or the slepton can have a non-zero lifetime. Combining several analyses, lower mass limits on $\tilde{\mu}_R$ of 96.3 GeV and on $\tilde{e}_R$ of 66 GeV are set for all slepton lifetimes at LEP [144]. In a considerable part of parameter space in these models, the $\tilde{\tau}$ is the NLSP. The LEP experiments have set lower limits on the mass of such a $\tilde{\tau}$ between 87 and 97 GeV, depending on the $\tilde{\tau}$ lifetime. ATLAS has searched for final states with τs, jets and missing transverse momentum, and has interpreted the results in GMSB models setting limits on the model parameters [145]. CMS has interpreted a multilepton analysis in terms of limits on gauge mediation models with slepton NLSP [146]. CDF has put limits on gauge mediation models at high $\tan\beta$ and slepton NLSP using an analysis searching for like-charge light leptons and taus [147].

Limits also exist on sleptons in R-parity violating models, both from LEP and the Tevatron experiments. From LEP, lower limits on $\tilde{\mu}_R$ and $\tilde{e}_R$ masses in such models are

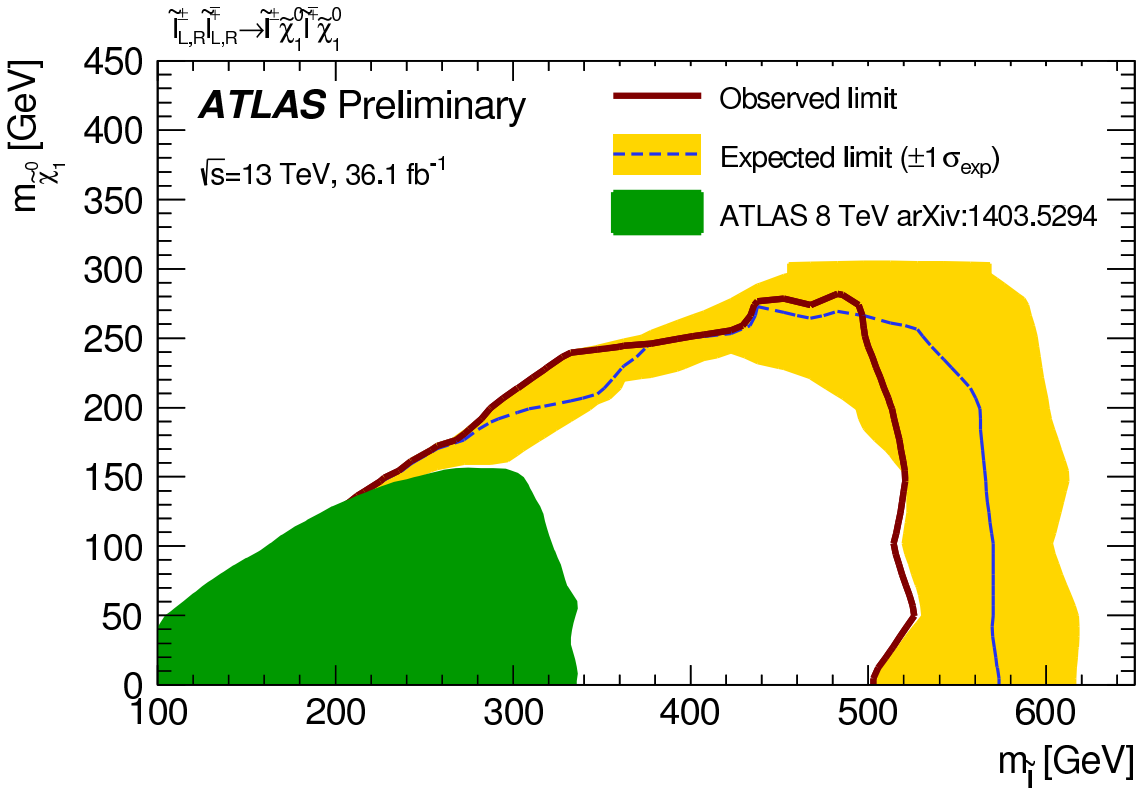

Figure 113.5: LHC exclusion limits on slepton (selectron and smuon) masses, assuming equal masses of selectrons and smuons, degeneracy of $\tilde{\ell}_{\rm L}$ and $\tilde{\ell}_{\rm R}$, and a 100% branching fraction for $\tilde{\ell} \to \ell\tilde{\chi}^0_1$ [118].

97 GeV, and the limits on the stau mass are very close: 96 GeV [148].

113.6.2. *Exclusion limits on sneutrino masses* :

The invisible width of the Z boson puts a lower limit on the sneutrino mass of about 45 GeV. Tighter limits are derived from other searches, notably for gauginos and sleptons, under the assumption of gaugino and sfermion mass universality at the GUT scale, and amount to approximately 94 GeV in the MSSM [149]. It is possible that the lightest sneutrino is the LSP; however, a left-handed sneutrino LSP is ruled out as a cold dark matter candidate [150,151].

Production of pairs of sneutrinos in R-parity violating models has been searched for at LEP [148]. Assuming fully leptonic decays via λ-type couplings, lower mass limits between 85 and 100 GeV are set. At the Tevatron [152,153] and at the LHC [154,155], searches have focused on scenarios with resonant production of a sneutrino, decaying to $e\mu$, $\mu\tau$ and $e\tau$ final states. No signal has been seen, and limits have been set on sneutrino masses as a function of the value of relevant RPV couplings. As an example, the LHC experiments exclude a resonant tau sneutrino with a mass below 1500 GeV for $\lambda_{312} > 0.07$ and $\lambda'_{311} > 0.01$.

The limits on sleptons in simplified models are summarized in Table 113.4.

Table 113.4: Summary of slepton mass limits from LEP and LHC, assuming R-parity conservation and 100% branching fraction for $\tilde{\ell} \to \ell\tilde{\chi}_1^0$. Masses in this table are provided in GeV.

Assumption	$m_{\tilde{\ell}}$
$\tilde{\mu}_R$, $\Delta m(\tilde{\mu}_R, \tilde{\chi}_1^0) > 10$	> 94
$\tilde{e}_R$, $\Delta m(\tilde{e}_R, \tilde{\chi}_1^0) > 10$	> 94
$\tilde{e}_R$, any Δm	> 73
$\tilde{\tau}_R$, $\Delta m((\tilde{\tau}_R, \tilde{\chi}_1^0) > 7$	> 87
$\tilde{\nu}_e$, $\Delta m(\tilde{e}_R, \tilde{\chi}_1^0) > 10$	> 94
$m_{\tilde{e}_{L,R}} = m_{\tilde{\mu}_{L,R}}$, $m_{\tilde{\chi}_1^0} \approx 0$	> 500
$m_{\tilde{\chi}_1^0} > \approx 270$	no LHC limit

113.7. Exclusion limits on long-lived sparticles

Long-lived sparticles arise in many different SUSY models. In particular in co-annihilation scenarios, where the NLSP and LSP are nearly mass-degenerate, this is rather common in order to obtain the correct Dark Matter relic density. Prominent examples are scenarios featuring $\tilde{\tau}$ co-annihilation, or models of SUSY breaking, e.g. minimal anomaly-mediated SUSY breaking, in which the appropriate Dark Matter density is obtained by co-annihilation of the LSP with an almost degenerate long-lived wino. However, in general, also other sparticles can be long-lived and it is desirable to establish a comprehensive search programme for these special long-lived cases, which lead to distinct experimental search signatures, including displaced vertices or disappearing tracks, etc.

Already in the past experiments performed dedicated searches for long-lived SUSY signatures, but with the absence of any experimental evidence for SUSY so far, it is expected that in the future even more effort and focus will be placed on SUSY scenarios involving long-lived sparticles. As for the interpretation of the canonical SUSY searches, also for long-lived scenarios simplified models are a convenient tool to benchmark these special cases (see e.g. [156,157]) .

In the following we give an overview of the most recent and relevant results for dedicated long-lived SUSY searches.

If the decay of gluinos is suppressed, for example if squark masses are high, gluinos may live longer than typical hadronization times. It is expected that such gluinos will hadronize to long-living strongly interacting particles known as R-hadrons. In particular, if the suppression of the gluino decay is highly significant, as in the case that the squark masses are much higher than the TeV scale, these R-hadrons can be (semi-)stable in collider timescales. Searches for such R-hadrons exploit the typical signature of stable charged massive particles in the detector. As shown in the upper left plot of Fig. 113.6, the CMS experiment excludes semi-stable gluino R-hadrons with masses below approximately 1.6 TeV [158]. The limits depend on the probability for gluinos to form bound states

known as gluinoballs, as these are neutral and not observed in the tracking detectors. Similar limits are obtained by the ATLAS experiment [159]. Limits ranging between 1 and 1.6 TeV are set in the scenario of R-hadron decays inside the detector, using dE/dx measurements and searches for displaced vertices, for $c\tau$ ranging from 1 mm to more than 10 m, as shown in Fig. 113.6 (bottom left).

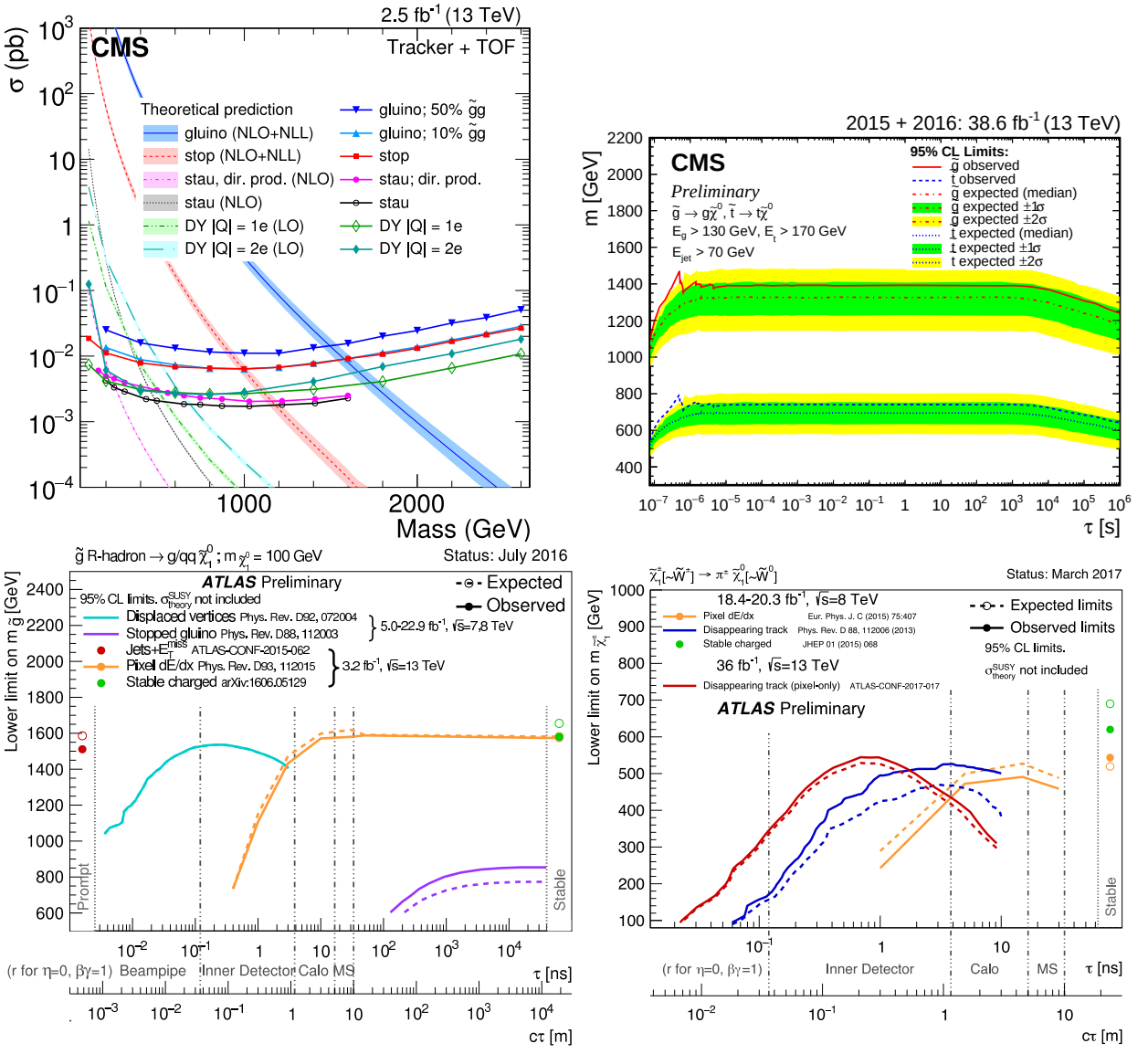

Figure 113.6: The upper left plot shows the observed 95% C.L. upper limits on the cross section for various long-lived charged sparticles. For gluinos, different fractions of gluinoball states produced after hadronization scenarios are indicated. The observed limits are compared with the predicted theoretical cross sections where the bands represent the theoretical uncertainties on the cross section values. The other plots show observed 95% C.L. lower limits on different sparticle masses in the mass-vs-lifetime plane for gluino R-hadrons (bottom left), stopped R-hadrons (top right) or charginos (bottom right).

Alternatively, since such R-hadrons are strongly interacting, they may be stopped in the calorimeter or in other material, and decay later into energetic jets. These decays are searched for by identifying the jets [160–162] or muons [163] outside the time window associated with bunch-bunch collisions. As shown in the upper right plot of Fig. 113.6, the CMS collaboration sets limits on such stopped R-hadrons over 13 orders of magnitude in gluino lifetime, up to masses of 1385 GeV [162]. A summary of a variety of different ATLAS searches for long-lived gluinos is shown in the lower left plot of Fig. 113.6. It displays constraints on the gluino mass-vs-lifetime plane for a split-supersymmetry model with the gluino R-hadron decaying into a gluon or light quarks and a neutralino with mass of 100 GeV.

Top squarks can also be long-lived and hadronize to a R-hadron, for example in the scenario where the top squark is the next-to-lightest SUSY particle (NLSP), with a small mass difference to the LSP. Searches for massive stable charged particles are sensitive to such top squarks. Displayed in the upper left plot of Fig. 113.6 are the results of the CMS analysis [158], which sets limits $m_{\tilde{t}} > 800$ GeV in such scenarios, while ATLAS [159] reports limits of $m_{\tilde{t}} > 900$ GeV. Limits from the Tevatron are about $m_{\tilde{t}} > 300$ GeV [164,165].

In addition to colored sparticles, also sparticles like charginos may be long-lived, especially in scenarios with compressed mass spectra. Charginos decaying in the detectors away from the primary vertex could lead to signatures such as kinked-tracks, or apparently disappearing tracks, since, for example, the pion in $\tilde{\chi}_1^{\pm} \to \pi^{\pm}\tilde{\chi}_1^0$ might be too soft to be reconstructed. At the LHC, searches have been performed for such disappearing tracks, and interpreted within anomaly-mediated SUSY breaking models [166–168]. The lower right plot of Fig. 113.6 shows constraints for different ATLAS searches on the chargino mass-vs-lifetime plane for an Anomaly Mediated SUSY Breaking (AMSB) model with $\tan\beta = 5$ and $\mu > 0$. It is assumed that wino-like charginos are pair-produced and decay to wino-like neutralinos and very soft charged pions. For example, for specific AMSB parameters, charginos with lifetimes between 0.1 and 10 ns are excluded for chargino masses up to 500 GeV. Within AMSB models, a lower limit on the chargino mass of 430 GeV is set, for a mass difference with the LSP of 160 MeV and a lifetime of 0.2 ns. Furthermore, charginos with a lifetime longer than the time needed to pass through the detector appear as charged stable massive particles. Limits have been derived by the LEP experiments [169], by D0 at the Tevatron [165], and by the LHC experiments [159,170,171]. For lifetimes above 100 ns, charginos below some 800 GeV are excluded.

In gauge mediation models, NLSP neutralino decays need not be prompt, and experiments have searched for late decays with photons in the final state. CDF have searched for delayed $\tilde{\chi}_1^0 \to \gamma\tilde{G}$ decays using the timing of photon signals in the calorimeter [172]. CMS has used the same technique at the LHC [173]. Results are given as upper limits on the neutralino production cross section as a function of neutralino mass and lifetime. D0 has looked at the direction of showers in the electromagnetic calorimeter with a similar goal [174], and ATLAS has searched for photon candidates that do not point back to the primary vertex, as well as for delayed photons [175].

Charged slepton decays may be kinematically suppressed, for example in the scenario

of a NLSP slepton with a very small mass difference to the LSP. Such a slepton may appear to be a stable charged massive particle. Interpretation of searches at LEP for such signatures within GMSB models with stau NLSP or slepton co-NLSP exclude masses up to 99 GeV [169]. Searches of stable charged particles at the Tevatron [164,165] and at the LHC [158,159] are also interpreted in terms of limits on stable charged sleptons. The limits obtained at the LHC exclude stable staus with masses below 240 GeV when produced directly in pairs, and below 490 GeV when staus are produced both directly and indirectly in the decay of other particles in a GMSB model [158].

113.8. Global interpretations

Apart from the interpretation of direct searches for sparticle production at colliders in terms of limits on masses of individual SUSY particles, model-dependent interpretations of allowed SUSY parameter space are derived from global SUSY fits. Typically these fits combine the results from collider experiments with indirect constraints on SUSY as obtained from low-energy experiments, flavor physics, high-precision electroweak results, and astrophysical data.

In the pre-LHC era these fits were mainly dominated by indirect constraints. Even for very constrained models like the CMSSM, the allowed parameter space, in terms of squark and gluino masses, ranged from several hundreds of GeV to a few TeV. Furthermore, these global fits indicated that squarks and gluino masses in the range of 500 to 1000 GeV were the preferred region of parameter space, although values as high as few TeV were allowed with lower probabilities [176].

With ATLAS and CMS now probing mass scales around 1 TeV and even beyond, the importance of the direct searches for global analyses of allowed SUSY parameter space has strongly increased. For example, imposing the new experimental limits on constrained supergravity models pushes the most likely values of first generation squark and gluino masses significantly beyond 2 TeV, typically resulting in overall values of fit quality much worse than those in the pre-LHC era [128]. Although these constrained models are not yet ruled out, the extended experimental limits impose very tight constraints on the allowed parameter space.

For this reason, the emphasis of global SUSY fits has shifted towards less-constrained SUSY models. Especially interpretations in the pMSSM [170,139–141] but also in simplified models have been useful to generalize SUSY searches, for example to redesign experimental analyses in order to increase their sensitivity for compressed spectra, where the mass of the LSP is much closer to squark and gluino masses than predicted, for example, by the CMSSM. As shown in Table 113.2, for neutralino masses above approximately 0.5 TeV the current set of ATLAS and CMS searches, interpreted in simplified models, cannot exclude the existence of squarks or gluinos with masses only marginally above the neutralino mass. However, as these exclusion limits are defined in the context of simplified models, they are only valid for the assumptions in which these models are defined.

As an alternative approach, both ATLAS [139] and CMS [140] have performed an analysis of the impact of their searches on the parameter space of the pMSSM. Fig. 113.7

shows graphically the LHC exclusion power in the pMSSM based on searches performed at $\sqrt{s} = 7$ and 8 TeV. The plot on the left shows the survival probability in the gluino-neutralino mass plane, which is a measure of the parameter space that remains after inclusion of the relevant CMS search results. As can be seen, gluino masses below about 1.2 TeV are almost fully excluded. This result agrees well with the typical exclusion obtained in simplified models for gluino production. However, as shown in the right plot of Fig. 113.7, when a similar analysis for other sparticles is performed it becomes apparent that exclusions on the pMSSM parameter can be significantly less stringent than simplified model limits might suggest. This is especially apparent for the electroweak sector, where even at rather low masses several of the pMSSM test points still survive the constraint of ATLAS searches at $\sqrt{s} = 7$ and 8 TeV. This again indicates that care must be taken when interpreting results from the LHC searches and there are still several scenarios where sparticles below the 1 TeV scale are not excluded, even when considering the most recent results at $\sqrt{s} = 13$ TeV.

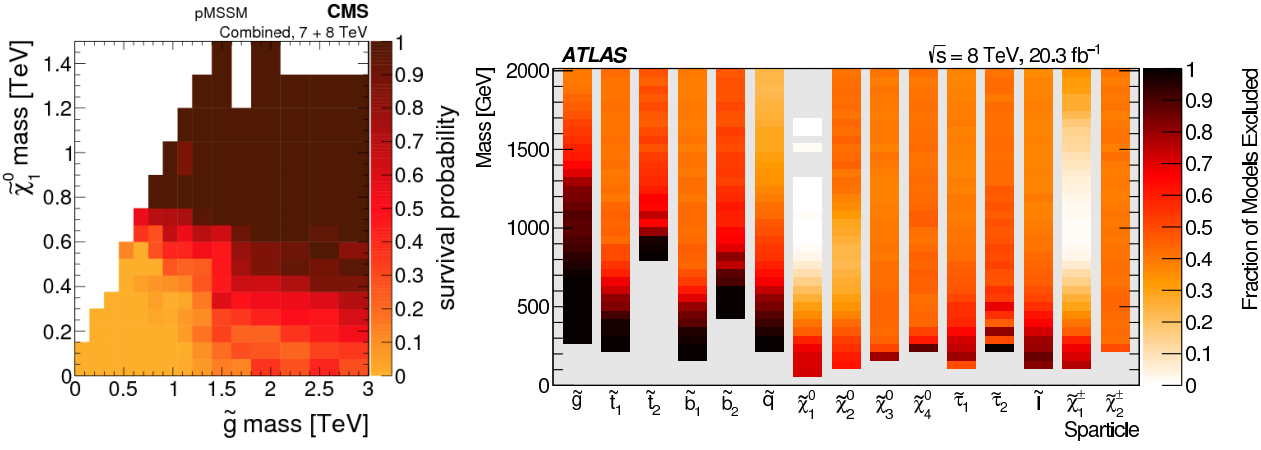

Figure 113.7: The plot on the left shows the survival probability of a pMSSM parameter space model in the gluino-neutralino mass plane after the application of the relevant CMS search results. The plot on the right shows a graphical representation of the ATLAS exclusion power in a pMSSM model. Each vertical bar is a one-dimensional projection of the fraction of models points excluded for each sparticle by ATLAS analyses. The experimental results are obtained from data taken at $\sqrt{s} = 7$ and 8 TeV.

Furthermore, the discovery of a Higgs boson with a mass around 125 GeV has triggered many studies regarding the compatibility of SUSY parameter space with this new particle. Much of it is still work in progress and it will be interesting to see how the interplay between the results from direct SUSY searches and more precise measurements of the properties of the Higgs boson will unfold in the future.

113.9. Summary and Outlook

The absence of any observation of new phenomena at the first run of the LHC at $\sqrt{s} = 7/8$ TeV, and now also during operation at $\sqrt{s} = 13$ TeV, place significant constraints on SUSY parameter space. Today, inclusive searches probe production of gluinos at about 2 TeV, first and second generation squarks in the range of about 1 to 1.6 TeV, third generation squarks at scales around 600 GeV to 1 TeV, electroweak gauginos at scales around $300 - 800$ GeV, and sleptons around 500 GeV. However, depending on the assumptions made on the underlying SUSY spectrum these limits can also weaken considerably.

Fig. 113.8 shows a comparison of the results from the first run of the LHC (about 20 fb^{-1} of data at $\sqrt{s} = 7/8$ TeV) with the new results obtained from about 36 fb^{-1} taken at $\sqrt{s} = 13$ TeV. Based on the example of a selected set of simplified model limits discussed in this review, it becomes apparent that for all sparticle sectors the new LHC results push sensitivity deep into new territory. This is especially apparent for limits on colored sparticles, which typically benefit most from the energy increase, but also limits on electroweakly produced sparticles have strengthened significantly since the last run period.

With the LHC having reached almost its maximum energy of about $\sqrt{s} = 14$ TeV, future sensitivity improvement will have to originate from more data and improvement of experimental analysis techniques. Therefore, it is expected that the current landscape of SUSY searches and corresponding exclusion limits at the LHC, as, for example, shown in Fig. 113.9 from the ATLAS experiment [177], will not change as rapidly anymore as it did in the past, when the LHC underwent several successive increases of collision energy.

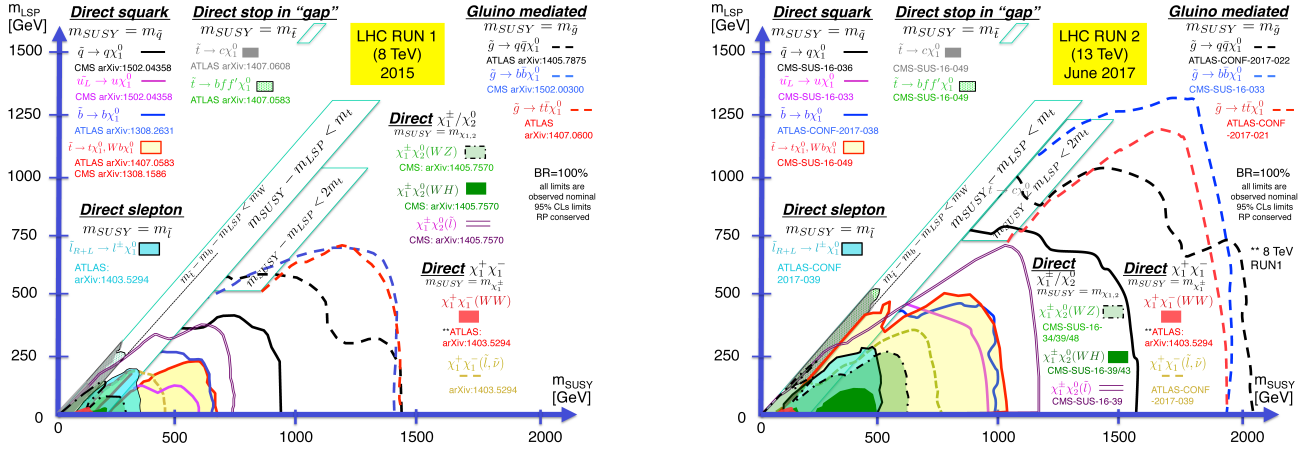

Figure 113.8: Comparison of a selected set of simplified model limits based on about 20 fb^{-1}) taken at $\sqrt{s} = 7/8$ TeV, with the same limits derived from 36 fb^{-1} taken at $\sqrt{s} = 13$ TeV. Further details about the different simplified models displaced here are provided in the text.

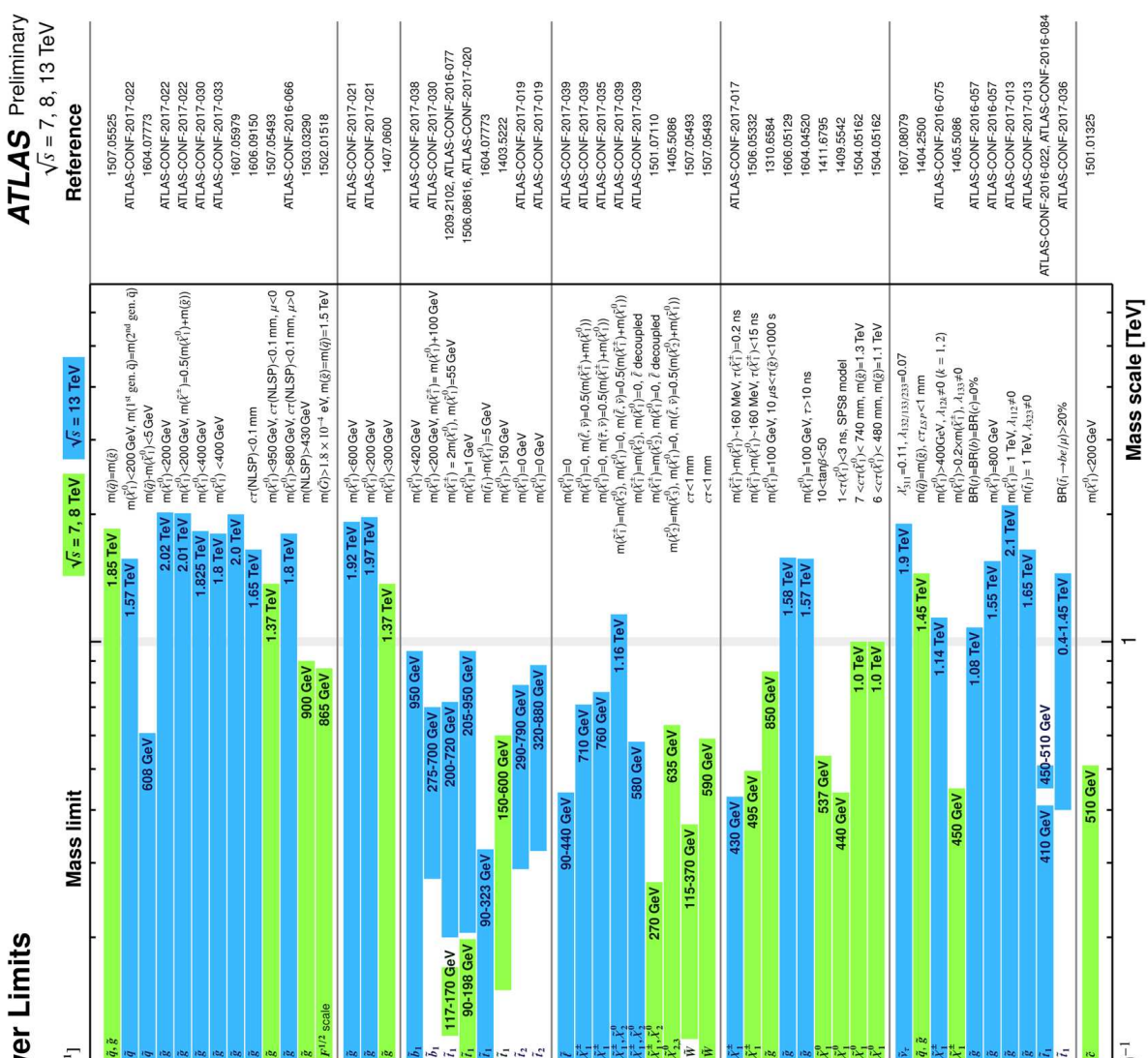

Figure 113.9: Overview of the current landscape of SUSY searches at the LHC. The plot shows exclusion mass limits of ATLAS for different searches and interpretation assumptions [177]. The corresponding results of the CMS experiment are similar [178].

The interpretation of results at the LHC has moved away from constrained models like the CMSSM towards a large set of simplified models, or the pMSSM. On the one hand this move is because the LHC limits have put constrained models like the CMSSM under severe pressure, while on the other hand simplified models leave more freedom to vary parameters and form a better representation of the underlying sensitivity of analyses. However, these interpretations in simplified models do not come without a price: the decomposition of a potentially complicated reality in a limited set of individual decay chains can be significantly incomplete. Therefore, quoted limits in simplified models are only valid under the explicit assumptions made in these models. The recent addition of more comprehensive interpretations in the pMSSM will complement those derived from simplified models and, thus, will enable an even more refined understanding of the probed SUSY parameter space.

In this context, the limit range of $1.5 - 2.0$ TeV on generic colored SUSY particles only holds for light neutralinos, in the R-parity conserving MSSM. Limits on third generation squarks and electroweak gauginos also only hold for light neutralinos, and under specific assumptions for decay modes and slepton masses.

The ongoing LHC run at $\sqrt{s} = 13$ TeV, and future runs at 14 TeV with significantly larger integrated luminosities (Run 3, and the High-Luminosity LHC), will provide a large data sample for future SUSY searches. As mentioned above, the improvement in sensitivity will largely have to come from the larger statistics, and evolution of trigger and analysis techniques, since there will be no significant energy increase at the LHC anymore. Although the sensitivity for colored sparticles will increase somewhat as well, the expanded data set will be particularly beneficial for electroweak gaugino searches, and for the more difficult final states presented by compressed particle spectra, stealth SUSY, long-lived sparticles, or R-parity violating scenarios.

References:

1. H. Miyazawa, Prog. Theor. Phys. **36**, 1266 (1966).
2. Yu. A. Golfand and E.P. Likhtman, Sov. Phys. JETP Lett. **13**, 323 (1971).
3. J.L. Gervais and B. Sakita, Nucl. Phys. **B34**, 632 (1971).
4. D.V. Volkov and V.P. Akulov, Phys. Lett. **B46**, 109 (1973).
5. J. Wess and B. Zumino, Phys. Lett. **B49**, 52 (1974).
6. J. Wess and B. Zumino, Nucl. Phys. **B70**, 39 (1974).
7. A. Salam and J.A. Strathdee, Nucl. Phys. **B76**, 477 (1974).
8. H.P. Nilles, Phys. Reports **110**, 1 (1984).
9. H.E. Haber and G.L. Kane, Phys. Reports **117**, 75 (1987).
10. E. Witten, Nucl. Phys. **B188**, 513 (1981).
11. S. Dimopoulos and H. Georgi, Nucl. Phys. **B193**, 150 (1981).
12. M. Dine, W. Fischler, and M. Srednicki, Nucl. Phys. **B189**, 575 (1981).
13. S. Dimopoulos and S. Raby, Nucl. Phys. **B192**, 353 (1981).
14. N. Sakai, Z. Phys. **C11**, 153 (1981).
15. R.K. Kaul and P. Majumdar, Nucl. Phys. **B199**, 36 (1982).
16. H. Goldberg, Phys. Rev. Lett. **50**, 1419 (1983).
17. J.R. Ellis *et al.*, Nucl. Phys. **B238**, 453 (1984).

18. G. Jungman and M. Kamionkowski, Phys. Reports **267**, 195 (1996).
19. S. Dimopoulos, S. Raby, and F. Wilczek, Phys. Rev. **D24**, 1681 (1981).
20. W.J. Marciano and G. Senjanović, Phys. Rev. **D25**, 3092 (1982).
21. M.B. Einhorn and D.R.T. Jones, Nucl. Phys. **B196**, 475 (1982).
22. L.E. Ibanez and G.G. Ross, Phys. Lett. **B105**, 439 (1981).
23. N. Sakai, Z. Phys. **C11**, 153 (1981).
24. U. Amaldi, W. de Boer, and H. Furstenau, Phys. Lett. **B260**, 447 (1991).
25. P. Langacker and N. Polonsky, Phys. Rev. **D52**, 3081 (1995).
26. P. Fayet, Phys. Lett. **B64**, 159 (1976).
27. G.R. Farrar and P. Fayet, Phys. Lett. **B76**, 575 (1978).
28. H.E. Haber, *Supersymmetry, Part I (Theory)*, in this *Review*.
29. CMS Collab. and LHCb Collab., Nature **522**, 68 (2015).
30. LHCb Collab., Phys. Rev. Lett. **118**, 191801 (2017).
31. A. Höcker and W.Marciano, *The Muon Anomalous Magnetic Moment*, in this *Review*.
32. G. Hinshaw *et al.*, Astrophys. J. Supp. **208**, 19H (2013).
33. Planck Collab., Astron. & Astrophys. **594**, A13 (2016).
34. M. Carena *et al.*, *Status of Higgs Boson Physics*, in this *Review*.
35. J.F. Grivaz, *Supersymmetry, Part II (Experiment)*, in: 2010 Review of Particle Physics, K. Nakamura *et al.*, (Particle Data Group), J. Phys. **G37**, 075021 (2010).
36. I. Hinchliffe *et al.*, Phys. Rev. **D55**, 5520 (1997).
37. L. Randall and D. Tucker-Smith, Phys. Rev. Lett. **101**, 221803 (2008).
38. CMS Collab., Phys. Lett. **B698**, 196 (2011).
39. CMS Collab., Phys. Rev. Lett. **107**, 221804 (2011).
40. CMS Collab., JHEP **1301**, 077 (2013).
41. CMS Collab., Eur. Phys. J. **C73**, 2568 (2013).
42. CMS Collab., Phys. Rev. **D85**, 012004 (2012).
43. C.G. Lester and D.J. Summers, Phys. Lett. **B463**, 99 (1999).
44. D.R. Tovey, JHEP **0804**, 034 (2008).
45. M.R. Buckley *et al.*, Phys. Rev. **D89**, 055020 (2014).
46. P. Jackson, C. Rogan, and M. Sartoni, Phys. Rev. **D95**, 035031 (2017).
47. J.M. Butterworth *et al.*, Phys. Rev. Lett. **100**, 242001 (2008).
48. A.H. Chamseddine, R. Arnowitt, and P Nath, Phys. Rev. Lett. **49**, 970 (1982).
49. E. Cremmer *et al.*, Nucl. Phys. **B212**, 413 (1983).
50. P. Fayet, Phys. Lett. **B70**, 461 (1977).
51. M. Dine, A.E. Nelson, and Yu. Shirman, Phys. Rev. **D51**, 1362 (1995).
52. P. Meade, N. Seiberg, and D. Shih, Prog. Theor. Phys. Supp. **177**, 143 (2009).
53. G.F. Giudice *et al.*, JHEP **9812**, 027 (1998).
54. L. Randall and R. Sundrum, Nucl. Phys. **B557**, 79 (1999).
55. R. Arnowitt and P Nath, Phys. Rev. Lett. **69**, 725 (1992).
56. G.L. Kane *et al.*, Phys. Rev. **D49**, 6173 (1994).
57. E. Halkiadakis, G. Redlinger, and D. Shih, Ann. Rev. Nucl. and Part. Sci. **64**, 319 (2014).
58. W. Beenakker *et al.*, Int. J. Mod. Phys. **A26**, 2637 (2011).

59. W. Beenakker *et al.*, Nucl. Phys. **B492**, 51 (1997); W. Beenakker *et al.*, Nucl. Phys. **B515**, 3 (1998); W. Beenakker *et al.*, Phys. Rev. Lett. **83**, 3780 (1999), Erratum *ibid.*, **100**, 029901 (2008); M. Spira, `hep-ph/0211145 (2002);`T. Plehn, Czech. J. Phys. 55, B213 (2005).
60. A. Djouadi, J-L. Kneur, and G. Moultaka, Comp. Phys. Comm. **176**, 426 (2007).
61. C.F. Berger *et al.*, JHEP **0902**, 023 (2009).
62. H. Baer *et al.*, `hep-ph/9305342`, 1993.
63. R.M. Barnett, H.E. Haber, and G.L. Kane, Nucl. Phys. **B267**, 625 (1986).
64. H. Baer, D. Karatas, and X. Tata, Phys. Lett. **B183**, 220 (1987).
65. J. Alwall, Ph.C. Schuster, and N. Toro, Phys. Rev. **D79**, 075020 (2009).
66. J. Alwall *et al.*, Phys. Rev. **D79**, 015005 (2009).
67. O. Buchmueller and J. Marrouche, Int. J. Mod. Phys. **A29**, 1450032 (2014).
68. LEP2 SUSY Working Group, ALEPH, DELPHI, L3 and OPAL experiments, note LEPSUSYWG/04-02.1, `http://lepsusy.web.cern.ch/lepsusy`.
69. CDF Collab., Phys. Rev. Lett. **102**, 121801 (2009).
70. D0 Collab., Phys. Lett. **B660**, 449 (2008).
71. ATLAS Collab. *Search for squarks and gluinos in final states with jets and missing transverse momentum using 36 fb^{-1} of $\sqrt{s} = 13$ TeV pp collision data with the ATLAS detector*, ATLAS-CONF-2017-022 (2017).
72. CMS Collab., *Search for new phenomena with the* M_{T2} *variable in the all-hadronic final state produced in proton-proton collisions at $\sqrt{s}$ =13 TeV*, `arXiv:1705.04650`(2017).
73. CMS Collab., Phys. Rev. **D96**, 032003 (2017).
74. ATLAS Collab., *Search for production of supersymmetric particles in final states with missing transverse momentum and multiple b-jets at $\sqrt{s} = 13$ TeV proton-proton collisions with the ATLAS detector*, ATLAS-CONF-2017-021 (2017).
75. CMS Collab., *Search for supersymmetry in pp collisions at $\sqrt{s} = 13$ TeV in the single-lepton final state using the sum of masses of large-radius jets*, `arXiv:1705.04673`(2017).
76. ATLAS Collab., *Constraints on promptly decaying supersymmetric particles with lepton-number- and R-parity-violating interactions using Run-1 ATLAS data*, ATLAS-CONF-2015-018 (2015).
77. CMS Collab., *Search for RPV SUSY in the four-lepton final state*, CMS-PAS-SUS-13-010 (2013).
78. ATLAS Collab., Phys. Rev. **D92**, 072004 (2015).
79. CDF Collab., Phys. Rev. Lett. **107**, 042001 (2011).
80. ATLAS Collab., *Search for massive supersymmetric particles in multi-jet final states produced in pp collisions at $\sqrt{s} = 13$ TeV using the ATLAS detector at the LHC*, ATLAS-CONF-2016-057 (2016).
81. ATLAS Collab., JHEP **1709**, 088 (2017).
82. CMS Collab., Phys. Lett. **B730**, 193 (2014).
83. CMS Collab., Phys. Lett. **B770**, 257 (2017).
84. ATLAS Collab,. Phys. Rev. Lett. **114**, 161801 (2015).
85. CDF Collab., Phys. Rev. Lett. **105**, 081802 (2010).

86. D0 Collab., Phys. Lett. **B693**, 95 (2010).
87. CMS Collab., *Search for the pair production of third-generation squarks with two-body decays to a bottom or charm quark and a neutralino in proton-proton collisions at* $\sqrt{s} = 13$ *TeV*, arXiv:1707.07274(2017).
88. ATLAS Collab., *Search for supersymmetry in events with b-tagged jets and missing transverse momentum in pp collisions at* $\sqrt{s} = 13$ *TeV with the ATLAS detector*, arXiv:1708.09266(2017).
89. ATLAS Collab., Eur. Phys. J. **C75**, 510 (2015).
90. CMS Collab., Eur. Phys. J. **C77**, 578 (2017).
91. C. Boehm, A. Djouadi, and Y. Mambrini, Phys. Rev. **D61**, 095006 (2000).
92. CDF Collab., Phys. Rev. **D82**, 092001 (2010).
93. D0 Collab., Phys. Lett. **B696**, 321 (2011).
94. CDF Collab., JHEP **1210**, 158 (2012).
95. D0 Collab., Phys. Lett. **B665**, 1 (2008).
96. CDF Collab., Phys. Rev. Lett. **104**, 251801 (2010).
97. D0 Collab., Phys. Lett. **B674**, 4 (2009).
98. CMS Collab., JHEP **1710**, 005 (2017).
99. CMS Collab., JHEP **1710**, 019 (2017).
100. ATLAS Collab., *Search for a scalar partner of the top quark in the jets+*$E_{\mathrm{T}}^{\mathrm{miss}}$ *final state at* $\sqrt{s} = 13$ *TeV with the ATLAS detector*, arXiv:1709.04183(2017).
101. ATLAS Collab., *Search for top squarks in final states with one isolated lepton, jets and missing transverse momentum using* 36.1 fb^{-1} *of* $\sqrt{s} = 13$ *TeV pp collision data with the ATLAS detector*, ATLAS-CONF-2017-037 (2017).
102. CMS Collab., *Search for direct stop pair production in the dilepton final state at* $\sqrt{s} = 13$ *TeV*, CMS-PAS-SUS-17-001 (2017).
103. ATLAS Collab., *Search for direct top squark pair production in final states with two leptons in* $\sqrt{s} = 13$ *TeV pp collisions with the ATLAS detector*, arXiv:1708.03247(2017).
104. ATLAS Collab., *Search for dark matter and other new phenomena in events with an energetic jet and large missing transverse momentum using the ATLAS detector*, ATLAS-CONF-2017-060 (2017).
105. H1 Collab., Eur. Phys. J. **C71**, 1572 (2011).
106. CMS Collab., Phys. Rev. **D91**, 052012 (2015).
107. ZEUS Collab., Eur. Phys. J. **C50**, 269 (2007).
108. CMS Collab., Phys. Rev. Lett. **111**, 221801 (2013).
109. ATLAS Collab., *A search for* $B - L$ *R-parity-violating scalar tops in* $\sqrt{s} = 13$ *TeV pp collisions with the ATLAS experiment*, arXiv:1710.05544(2017).
110. CMS Collab., Phys. Rev. Lett. **114**, 061801 (2015).
111. CMS Collab., Phys. Lett. **B760**, 178 (2016).
112. ATLAS Collab., *A search for pair-produced resonances in four-jet final states at* $\sqrt{s} = 13$ *TeV with the ATLAS detector*, ATLAS-CONF-2017-025 (2017).
113. CMS Collab., Phys. Lett. **B747**, 98 (2015).
114. LEP2 SUSY Working Group, ALEPH, DELPHI, L3 and OPAL experiments, note LEPSUSYWG/01-03.1, http://lepsusy.web.cern.ch/lepsusy.

115. LEP2 SUSY Working Group, ALEPH, DELPHI, L3 and OPAL experiments, note LEPSUSYWG/02-04.1, `http://lepsusy.web.cern.ch/lepsusy`.
116. CDF Collab., *Search for trilepton new physics and chargino-neutralino production at the Collider Detector at Fermilab*, CDF Note 10636 (2011).
117. D0 Collab., Phys. Lett. **B680**, 34 (2009).
118. ATLAS Collab. *Search for electroweak production of supersymmetric particles in the two and three lepton final state at* $\sqrt{s} = 13$ *TeV with the ATLAS detector*, ATLAS-CONF-2017-039 (2017).
119. ATLAS Collab., JHEP **1405**, 071 (2014).
120. CMS Collab., *Search for electroweak production of charginos and neutralinos in multilepton final states in pp collision data at* $\sqrt{s} = 13$ *TeV*, `arXiv:1709.05406`(2017).
121. ATLAS Collab., *Search for the direct production of charginos and neutralinos in* $\sqrt{s} = 13$ *TeV pp collisions with the ATLAS detector*, `arXiv:1708.07875`(2017).
122. CMS Collab., *Combined search for electroweak production of charginos and neutralinos in pp collisions at* $\sqrt{s} = 13$ *TeV*, CMS-PAS-SUS-17-004 (2017).
123. ATLAS Collab., Eur. Phys. J. **C75**, 208 (2015).
124. ATLAS Collab., Phys. Rev. **D93**, 052002 (2016).
125. CMS Collab., JHEP **1511**, 189 (2015).
126. H. Dreiner *et al.*, Eur. Phys. J. **C62**, 547 (2009).
127. LEP2 SUSY Working Group, ALEPH, DELPHI, L3 and OPAL experiments, note LEPSUSYWG/04-07.1, `http://lepsusy.web.cern.ch/lepsusy`.
128. For a sampling of recent post-LHC global analyses, see: GAMBIT Collab, arXiv:1705.07935; E.A. Bagnaschi *et al.*, Eur. Phys. J. **C77**, 268 (2017); E.A. Bagnaschi *et al.*, Eur. Phys. J. **C77**, 104 (2017); P. Bechtle *et al.*, Eur. Phys. J. **C76**, 9, (2016); E.A. Bagnaschi *et al.*, Eur. Phys. J. **C75**, 500 (2015); O. Buchmueller *et al.*, Eur. Phys. J. **C74**, 3212 (2014); O. Buchmueller *et al.*, Eur. Phys. J. **C74**, 2922 (2014); M. Citron *et al.*, Phys. Rev. **D87**, 036012 (2013); C. Strege *et al.*, JCAP **1304**, 013 (2013); A. Fowlie *et al.*, Phys. Rev. **D86**, 075010 (2012).
129. LEP2 SUSY Working Group, ALEPH, DELPHI, L3 and OPAL experiments, note LEPSUSYWG/04-09.1, `http://lepsusy.web.cern.ch/lepsusy`.
130. CDF Collab., Phys. Rev. Lett. **104**, 011801 (2010).
131. D0 Collab., Phys. Rev. Lett. **105**, 221802 (2010).
132. ATLAS Collab., Eur. Phys. J. **C76**, 517 (2016).
133. CMS Collab., *Search for supersymmetry in events with at least one photon, missing transverse momentum, and large transverse event activity in proton-proton collisions at* $\sqrt{s} = 13$ *TeV*, `arXiv:1707.06193`(2017).
134. ATLAS Collab., Eur. Phys. J. **C77**, 144 (2017).
135. CMS Collab., Phys. Rev. **D90**, 092007 (2014).
136. CMS Collab., JHEP **04**, 124 (2016).
137. ATLAS Collab., *Search for supersymmetry in events with four or more leptons in* $\sqrt{s} = 13$ *TeV pp collisions using* 13.3 fb^{-1} *of ATLAS data*, ATLAS-CONF-2016-075 (2016).
138. CMS Collab., Phys. Rev. **D91**, 012007 (2015).

139. ATLAS Collab., JHEP **1510**, 134 (2015).
140. CMS Collab., JHEP **1610**, 129 (2016).
141. For a sampling of recent pMSSM analyses, see: GAMBIT Collab, arXiv:1705.07917; K. de Vries *et al.*, Eur. Phys. J. **C75**, 422 (2015); C. Strege *et al.*, JHEP **1409**, 081 (2014); M. Cahill-Rowley *et al.*, Phys. Rev. **D88**, 035002 (2013); C. Boehm *et al.*, JHEP **1306**, 113, (2013); S AbdusSalam, Phys. Rev. **D87**, 115012 (2013); A. Arbey *et al.*, Eur. Phys. J. **C72**, 2169 (2012); A. Arbey *et al.*, Eur. Phys. J. **C72**, 1847 (2012); M. Carena *et al.*, Phys. Rev. **D86**, 075025 (2012); S. Sekmen *et al.*, JHEP **1202**, 075 (2012).
142. LEP2 SUSY Working Group, ALEPH, DELPHI, L3 and OPAL experiments, note LEPSUSYWG/04-01.1, `http://lepsusy.web.cern.ch/lepsusy`.
143. ALEPH Collab., Phys. Lett. **B544**, 73 (2002).
144. LEP2 SUSY Working Group, ALEPH, DELPHI, L3 and OPAL experiments, note LEPSUSYWG/02-09.2, `http://lepsusy.web.cern.ch/lepsusy`.
145. ATLAS Collab., JHEP **1409**, 103 (2014).
146. CMS Collab., Phys. Rev. **D90**, 032006 (2014).
147. CDF Collab., Phys. Rev. Lett. **110**, 201802 (2013).
148. LEP2 SUSY Working Group, ALEPH, DELPHI, L3 and OPAL experiments, note LEPSUSYWG/02-10.1, `http://lepsusy.web.cern.ch/lepsusy`.
149. DELPHI Collab., Eur. Phys. J. **C31**, 412 (2003).
150. T. Falk, K.A. Olive, and M. Srednicki, Phys. Lett. **B339**, 248 (1994).
151. C. Arina and N. Fornengo, JHEP **0711**, 029 (2007).
152. CDF Collab., Phys. Rev. Lett. **105**, 191801 (2010).
153. D0 Collab., Phys. Rev. Lett. **105**, 191802 (2010).
154. ATLAS Collab., Phys. Rev. Lett. **115**, 031801 (2015).
155. CMS Collab., Eur. Phys. J. **C76**, 317 (2016).
156. O. Buchmueller *et al.*, *Simplified Models for Displaced Dark Matter Signatures*, `arXiv:1704.06515`.
157. V. Khoze *et al.*, JHEP **06**, 041 (2017).
158. CMS Collab., Phys. Rev. **D94**, 112004 (2016).
159. ATLAS Collab., Phys. Lett. **B760**, 647 (2016).
160. D0 Collab., Phys. Rev. Lett. **99**, 131801 (2007).
161. ATLAS Collab., Phys. Rev. **D88**, 112003 (2013).
162. CMS Collab., *Search for stopped long-lived particles produced in pp collisions at* $\sqrt{s} = 13$ *TeV*, CMS-PAS-EXO-16-004 (2017).
163. CMS Collab., *Search for long-lived particles that stop in the CMS detector and decay to muons at* $\sqrt{s} = 13$ *TeV*, CMS-PAS-EXO-17-004 (2017).
164. CDF Collab., Phys. Rev. Lett. **103**, 021802 (2009).
165. D0 Collab., Phys. Rev. **D87**, 052011 (2013).
166. ATLAS Collab., Phys. Rev. **D88**, 112006 (2013).
167. ATLAS Collab., *Search for long-lived charginos based on a disappearing-track signature in pp collisions at* $\sqrt{s} = 13$ *TeV with the ATLAS detector*, ATLAS-CONF-2017-017 (2017).
168. CMS Collab., JHEP **1501**, 096 (2015).

169. LEP2 SUSY Working Group, ALEPH, DELPHI, L3 and OPAL experiments, note LEPSUSYWG/02-05.1, `http://lepsusy.web.cern.ch/lepsusy`.
170. CMS Collab., Eur. Phys. J. **C75**, 325 (2015).
171. LHCb Collab., Eur. Phys. J. **C75**, 595 (2015).
172. CDF Collab., Phys. Rev. **D88**, 031103 (2013).
173. CMS Collab., Phys. Lett. **B722**, 273 (2013).
174. D0 Collab., Phys. Rev. Lett. **101**, 111802 (2008).
175. ATLAS Collab, Phys. Rev. **D90**, 112005 (2014).
176. For a sampling of pre-LHC global analyses, see: O. Buchmueller *et al.*, Eur. Phys. J. **C71**, 1722 (2011); E.A. Baltz and P. Gondolo, JHEP **0410**, 052 (2004); B.C. Allanach and C.G. Lester, Phys. Rev. **D73**, 015013 (2006); R.R. de Austri *et al.*, JHEP **0605**, 002 (2006); R. Lafaye *et al.*, Eur. Phys. J. **C54**, 617 (2008); S. Heinemeyer *et al.*, JHEP **0808**, 08 (2008); R. Trotta *et al.*, JHEP **0812**, 024 (2008); P. Bechtle *et al.*, Eur. Phys. J. **C66**, 215 (2010).
177. Supersymmetry Physics Results, ATLAS experiment, `http://twiki.cern.ch/twiki/bin/view/AtlasPublic/SupersymmetryPublicResults/`.
178. Supersymmetry Physics Results, CMS experiment, `http://cms-results.web.cern.ch/cms-results/public-results/publications/SUS/index.html`.